Late Neogene evolution of the Peruvian margin and its ecosystems: A synthesis from the Sacaco record

Supplementary Online Material

Diana Ochoa*[,a], Rodolfo Salas-Gismondi [a, b], Thomas J. DeVries [c], Patrice Baby [d], Christian de Muizon [e], Alí Altamirano [b], Angel Barbosa-Espitia [f,g], David A. Foster [f], Kelly Quispe [h], Jorge Cardich [a], Dimitri Gutierrez [h,i], Alexander Perez [a,], Juan Valqui [a], Mario Urbina [b], Matthieu Carré [a,j]

[a] Laboratorios de Investigación y Desarrollo (LID), Centro de Investigación para el Desarrollo Integral y Sostenible (CIDIS), Facultad de Ciencias y Filosofía, Universidad Peruana Cayetano Heredia, Av. Honorio Delgado 430, Lima, Peru
ORCID: 0001-6242-4202

[b] Departamento de Paleontología de Vertebrados, Museo de Historia Natural, Universidad Nacional Mayor de San Marcos, Lima, Peru

[c] Burke Museum of Natural History and Culture, University of Washington, Seattle, Washington 98195, USA

[d] Géosciences-Environnement Toulouse, UMR CNRS/IRD/Université Paul Sabatier, 14 Avenue Edouard Belin, 31400 Toulouse, France

[e] CR2P (CNRS, MNHN, Sorbonne Université), Département Origines et Évolution, Muséum national d'Histoire naturelle, case postale 38, 57 rue Cuvier, F-75231 Paris cedex 05, France

[f] Department of Geological Sciences, University of Florida, 241 Williamson Hall, Gainesville, Florida 32611, USA

[g] Instituto de Investigaciones en Estratigrafía (IIES), Universidad de Caldas, Calle 65 # 26-10, edificio Orlado Sierra, Bloque B, segundo piso, Manizales, Colombia

[h] Programa de Maestría en Ciencias del Mar, Universidad Peruana Cayetano Heredia, Lima, Peru

[i] Instituto del Mar del Peru (IMARPE), Dirección de Investigaciones Oceanográficas, Callao, Peru

[j] LOCEAN Laboratory, Sorbonne Université (UPMC)-CNRS-IRD-MNHN, Paris, France

Table of Contents

1. *Existing geological data and field observations*

Existing chronostratigraphic constraints for the northern East Pisco Basin (EPB) and the Sacaco sub-basin, including radiometric, isotopic and (bio)stratigraphic information, are summarized in the Table S1. A complete list of all vertebrate fossils reported from each locality with corresponding references can be found in the Table S2.

Field observations were made at the Sacaco sub-basin, close to the villages of Yauca and Chaviña (Arequipa Department). Stratigraphic sections were logged and sampled at the Sacaco, Yauca, Cerro Amarillo, and Quebrada Caracoles localities (Fig. S1).

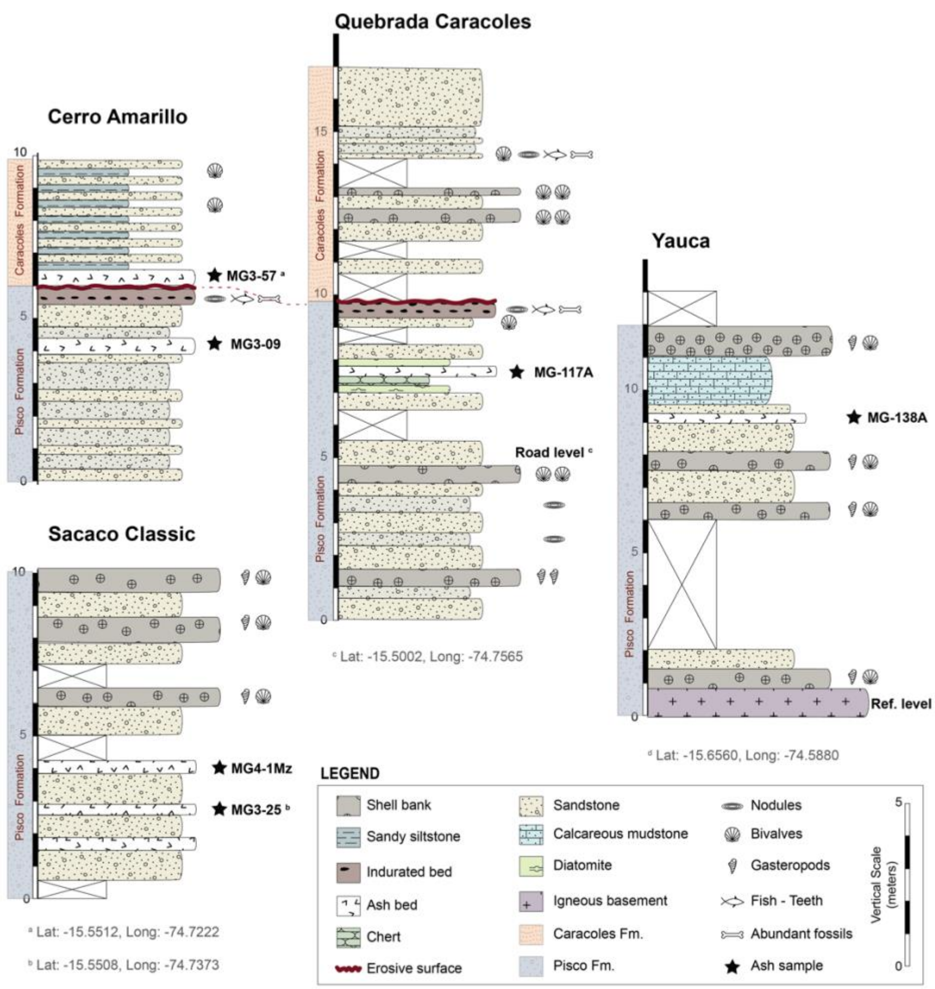

Fig. S1. Stratigraphic logs of Cerro Amarillo, Sacaco Classic, Quebrada Caracoles, and Yauca localities. Logs show distribution of the Pisco and Caracoles formations with brief lithological descriptions, fossil beds, and location of six tuff sampled for radiometric dating. Note that MG4- 1Mz was obtained from the same tuff sampled by Muizon and Bellon (1980) in the Sacaco locality. For each stratigraphic section a referential location (latitude and longitude) in the field is indicated, and their geographic position is shown in Fig. 3A.

- ***Sacaco locality:***

The Sacaco locality is situated east of the South Panamerican Highway 1S, between the villages of Puerto Lomas and Chaviña (Fig. 3A-B). This locality is also known as "*Sacaco Chacra" or "Sacaco Classic*". The Sacaco stratigraphic section is primarily composed of a thick yellow marine medium-grained sandy sequence, intercalated with grey fine-grained tuffaceous sandstones, at least three well-developed tuff levels, and several one to three meter-thick banks formed by bivalve shells of *Anadara chilensis* and *Dosinia ponderosa* (SB in Figs. 3B and S1). The medium-grain sandstone beds are up to 1 m thick, structureless, moderately cemented, poorly sorted, and mainly composed of quartz, with biotite, pyroxene, and volcanic glass as main accessory minerals. By contrast, the grey fine-grained sandstone levels are massive, very well cemented, well sorted, and consists of quartz and volcanic glass.

The most characteristic vertebrate fossils found in the Pisco Formation at the Sacaco locality include aquatic sloths (*Thalassocnus carolomartini*), phocid pinnipeds (*Acrophoca longirostris*, *Piscophoca pacifica)*, porpoises (*Piscolithax longirostris)*, walrus-like dolphin (*Odobenocetops leptodon)*, delphinid dolphins (*Stenella* sp., cf. *Delphinus* sp.), large-sized sharks (*Carcharocles megalodon*, *Carcharodon carcharias*), penguins (*Spheniscus urbinai*), and crocodylians (*Piscogavialis jugaliperforatus)*.

- ***Yauca locality:***

The succession is located at the southernmost edge of the sub-basin, between the villages of Chaviña and Yauca (Fig. 3A). Given its location close to the present-day coast, this section is strongly affected by winds that cover most of the rock exposures with sand. Sediments from the Pisco Formation at Yauca unconformably sit over igneous basement from the Proterozoic Coastal Basal Complex. The section consists of at least four prominent and indurated shell banks of up to 1 m thick with local lateral variations to well-cemented, bio-supported whitish sandstone beds containing articulated and disarticulated bivalves and barnacles (SB 1-4 in Fig. 3E). Shell banks intercalate with immature grey medium-to-coarse sand beds, that are massive, poorly cemented, and moderately sorted (Fig. 5G). Compositionally, these sandstones are formed by grains of quartz (70%), feldspars (15%), biotite (~3-5%), pyroxene (~3%), lithic fragments (~5%), and bioclastic debris (~3-5%). Bioturbation marks and fossil remains, such as vertebrate bones and teeth, commonly occur in these grey sands. Some minor shell banks and lenses of discrete thicknesses (less than 10 centimeters) irregularly occur within the grey sand beds, but are not included in the shell bank numbering (SB 1-4 in Fig. 3E). Towards the top of the exposed succession, the grey medium-to-coarse sandstones gradate to very fine- to fine-grained indurated sandy beds. The main vertebrate fossil remains unearthed from the Pisco Formation in Yauca include aquatic sloths (*Thalassocnus yaucensis*), gavialoid crocodylians (*Piscogavialis jugaliperforatus*), walrus-like dolphins (*Odobenocetops* cf. *leptodon*), large-sized sharks (*Carcharocles megalodon, Carcharodon carcharias*), and penguins

(*Spheniscus urbinai*). Further details can be found in Table S2.

- ***Cerro Amarillo locality:***

The Cerro Amarillo locality is situated east of the South Panamerican Highway 1S between the small towns of Puerto Lomas and Chaviña, 1.5 kilometers to the southeast of Sacaco (Fig. 3A-C). The succession was measured at the mouth of an intermittent stream locally known as *Toro Muerto*. The Cerro Amarillo hill, after which the locality is named, provides one of the best rock exposures of the upper Pisco and lower Caracoles formations at the Sacaco sub-basin (Fig. 3C). The Pisco Formation mainly consists of alternating fine-to-medium-grained mature sands and tuffaceous sandy beds. There are at least three well-defined tuff beds located towards the upper half of the section (Fig. S1). Sandstones are organized in white to yellow-colored, massive to parallel-laminated beds of up to 30 centimeters thick, composed of quartz with large-size biotite and pyroxene crystals. It is common to find disarticulated, but complete, bivalve shells of *Dosinia* sp. and *Anadara* sp. Towards the top, these sands are replaced by an indurated sandstone bed containing abundant phosphate nodules, shark and ray teeth, and broken bones (Fig. S1). The top of this indurated bed corresponds to an erosional surface marking the end of the Pisco Formation at the Cerro Amarillo area (Fig. 3C). A 30-50 centimeters thick tuff bed occurs close to the top of the succession (MG3-09 in Fig. 3C and S1). The Caracoles Formation comprises dark olive massive to parallel laminated silts or sandy silts, interbedded with grey to yellowish fine-grained sandstones, and occasional centimeter-thick diatomaceous levels, blackish siltstones and thin shells banks. Near the base of the formation, a 20 centimeters thick tuff bed occurs (MG3-57 in Fig. 3C and S1). Throughout the unit, and especially associated with the sandstone beds, it is common to find vertebrate bones, shark and fish remains (teeth, scales), bryozoans, and shells of bivalves (e.g., *Pitar* sp., *Mulinia* sp., *Polinices* sp.) and gastropods (e.g., *Nassarius* sp., *Cancellaria* sp.). To date, the existing vertebrate fossil material from this locality is part of the MUSM collection and has not been published (Table S2). Internal MUSM reports document the presence of delphinid dolphins (Delphinidae indet., MUSM 3595), otariid pinnipeds (MUSM 3736 and MUSM 3701), sharks (e.g., *Carcharodon carcharias*, *Galeorhinus* sp., *Carcharhinus* sp.), filefish (*Aluterus* sp.) and rays.

- ***Quebrada Caracoles locality :***

The succession is located along an intermittent stream with the same name, 10 km WSW of the Bella Union Village (Fig. 3A). The base of the section starts at the mouth of the stream and continues upstream. The Pisco Formation mainly consists of medium-grained olive sandstones, intercalated with thin fine-grained grey indurated sand beds, tuffaceous sandstones, shell banks, and thin layers of chert and diatomaceous mudstone (Fig. S1). Olive sandstone beds, weathering to yellowish colors, are moderately cemented, and generally structureless with normal grading and frequent bioturbation. The beds are composed of moderate to well sorted, subangular grains of quartz (70%), feldspars (10-

20%), lithic fragments (~5-10%), micas (~2%), heavy minerals (~1-2%), with a variable content of shells fragments. By contrast, the grey sands are well-cemented, massive to nodular-bedded, non-bioturbated, and are constituted by quartz (80%), feldspars (10%), heavy minerals (~5%), micas (2 %), and lithic fragments (1 %). Close to the mouth of the stream, two conspicuous shell banks occur, a lower one dominated by the turritellid *Turritella cingulatiformis*, and about five meters above, another comprised of *Mulinia* and *Pitar* valves (DeVries, 2020).

The Caracoles Formation is generally well-exposed across the course the *Quebrada Caracoles*, reaching a total thickness of about 30 meters. The lowermost part of the Caracoles Formation consists of olive to brown well-cemented sandstones, arranged in tabular bodies without evidence of bioturbation, but with common occurrences of bivalve fragments and molds. Locally, some layers are indurated and form nodular sand structures, often accompanied by fish and vertebrate remains. Upwards, the presence of bioclasts (mainly bivalve shells) increases and sandstone beds develop bioclastic lenses that gradually become well-developed coquina layers of up to five centimeters thick (Fig. S1). The same pattern persists until interrupted by an erosional unconformity that separates the Caracoles Formation from the overlying Pongo Formation (DeVries, 2020).

The most common vertebrate fossil remains recovered from the Pisco Formation in the Caracoles locality are sperm whales (Physeteridae indet.), dwarf sperm whales (*Scaphokogia* sp.), rorquals (*Balaenoptera* sp.), walrus-like dolphins (*Odobenocetops* sp.), and sharks (*Carcharodon carcharias*) (Table S2). The paleontological record from the Caracoles Formation includes large-sized sharks (*Carcharodon carcharias*), otariids (cf. *Hydrarctos*), an odobenid pinniped (MUSM 3719, MUSM 3620), delphinid dolphins (*Stenella* sp., MUSM 3906), and filefish (*Aluterus* sp.) (Table S2). As in the Cerro Amarillo section, the fossil vertebrate record from the Caracoles Formation recovered from this locality has not been published yet; fossils are currently housed at the MUSM.

2. *Zircon U-Pb geochronology methods*

Zircon U/Pb analyses were carried out at the Department of Geological Sciences of the University of Florida (DGS-UF). Crystals were isolated from a 2 kg sample using standard procedures, including rock disaggregation, gravimetric and magnetic separation methods, and handpicking. Only euhedral, colorless grains lacking visible inclusions were chosen for analysis. In all samples, a population of 40 zircon crystals was analyzed.

Zircon grains were separated from rock samples using standard procedures that include crushing, pulverizing, washing, sieving, gravimetric (water table and heavy liquids TBE and MeI) and magnetic susceptibility (Frantz® Isodynamic). Zircon crystals were handpicked and placed onto double-sided tape, mounted in an epoxy plug together with FC-1 zircon standard, and polished to expose the internal portion of the grains.

Cathodoluminescence (CL) imaging was performed using a Scanning Electron Microscope (SEM) with a Gatan® mini CL detector to decipher internal zonation patterns and the overall internal structure-texture of the sectioned grains (Fig. S2). Before laser ablation, the epoxy plugs were cleaned in an ultrasonic bath with diluted HNO3 to remove surface contamination. Analyses were carried out using a Nu-Plasma® Laser Ablation Multi-Collector Inductively Coupled Plasma Mass Spectrometer (LA-MC-ICP-MS). Mounted zircon grains were ablated with a New Wave 213 nm ultraviolet laser, using a laser spot size of 20 µm. Ar and He carrier gas was used for sample transport into the mass spectrometer. Background measurement for 20 seconds was performed before each ablation for blank correction and contribution from 204Hg, a common impurity in liquefied argon. Following this on peak zero, each sample was ablated for 30s at intervals of 10 unknown zircons, directly preceded and followed by ablation of two FC-1 standard zircon.

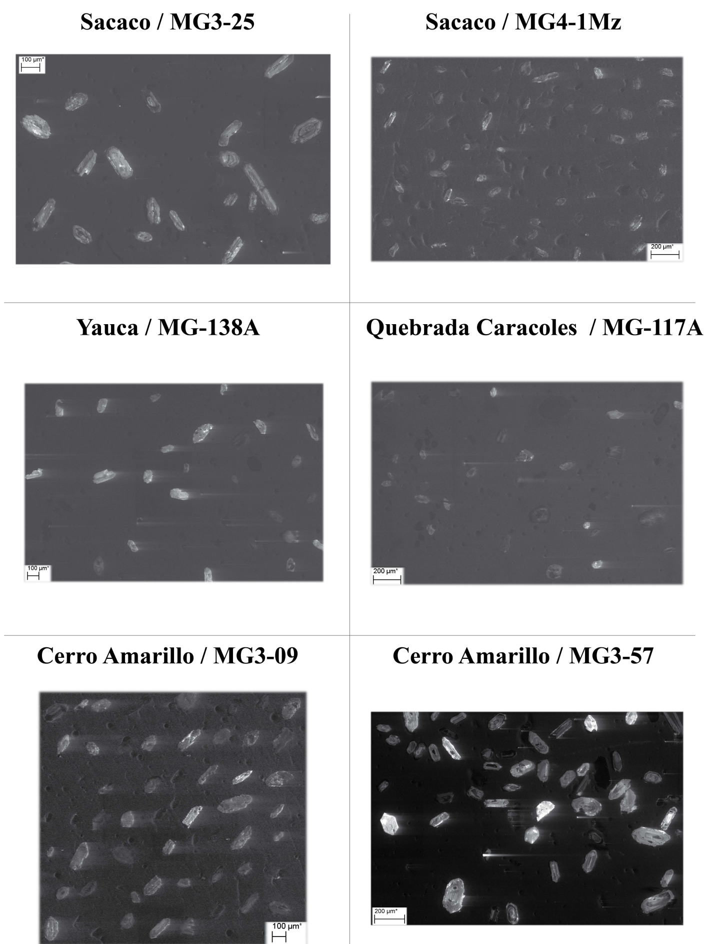

Fig. S2. Cathodoluminescence images of zircon grains from tuff samples showing internal textures (parameters EHT= 15.00 kV; WD= 16.0 mm; signal A= CL Detector).

Data reduction was referenced to standard zircon (FC-1) from the Duluth Gabbro dated at 1099.0 ± 0.7 Ma and 1099.1 ± 0.5 Ma (Black et al., 2004). Single-ages were calculated in Microsoft Excel using CALAMARI (in-house spreadsheet). The Isoplot package (Figs. S3 and S4; Vermeesch, 2018) from the open-source R program (R-Core Team, 2013) was also used to calculate the weighted mean age. Table S3 includes LA-MC-ICP-MS data and U/Pb calculated weighted mean ages for all zircons selected in each sample.

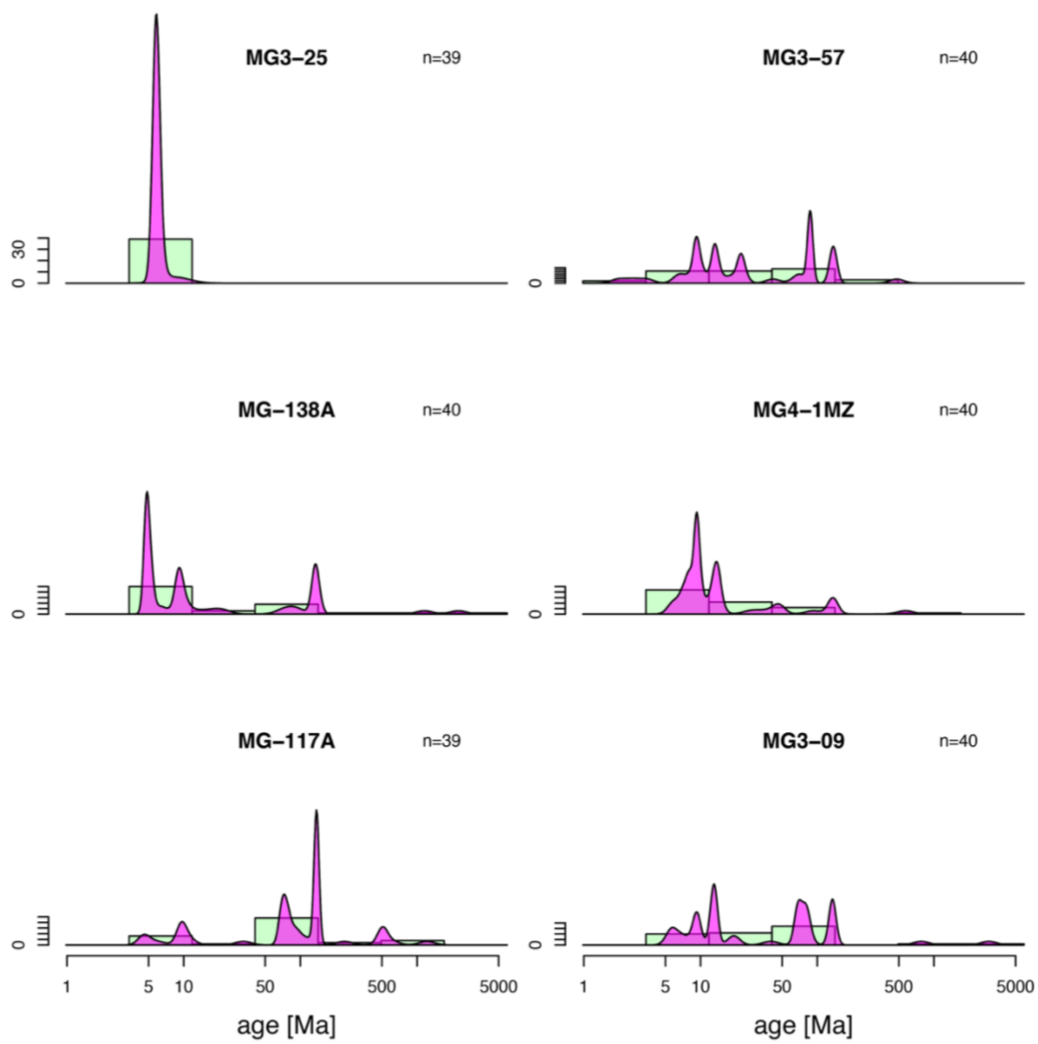

Fig. S3. Kernel density estimation (pink) and histogram plots (green rectangles) for U-Pb estimated zircon ages for the Sacaco sub-basin samples. Statistical treatment and graphic presentation after Vermeesch (2018).

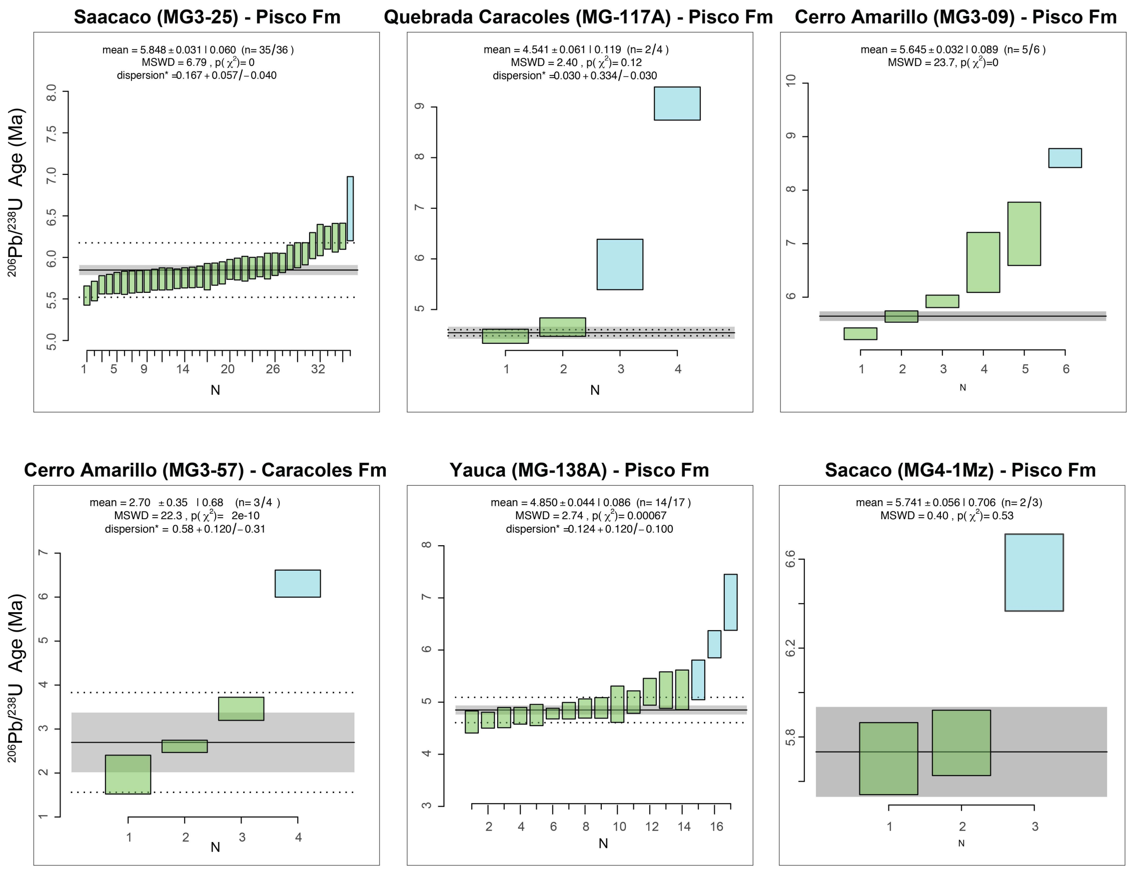

Grey bands represent confidence interval for μ
* Normal confidence region for the dispersion is shown as a set of dashed lines.

Fig. S4. U/Pb weighted mean ages for the collected tuff samples from the Sacaco sub-basin. Legend: mean = μ±x | y (| z); where: μ: the weighted mean age, x: the standard error (σ) of μ, y: the width of the 100(1-α) % confidence interval for μ (shown as a grey band on the plot). z: the approximate 100(1-α)% confidence interval for t with overdispersion, calculated as z = y√MSWD (Mean Square of the Weighted Deviates).

3. Analyses of the vertebrate paleontological record

- *Compilation of existing vertebrate paleontological data*

Vertebrate paleontological data (exclusive of non-tetrapod Osteichthyes) was gathered from 20 localities across the EPB (Table S2). This diverse 18-My-long faunal record allows describing original biological signals and diversity patterns of the pre-HCS ecosystems in relation to climatic and tectonic events, reducing preservational and sampling-related biases that occur when considering only individual fossiliferous localities. Compiled information encompasses published records as well as unpublished data (including unpublished theses, descriptions and archives from the Natural History Museum of the UNMSM [MUSM] in Lima, Peru). Unpublished paleontological occurrences were considered here only if they include complete location data and a repository number, regardless of their taxonomic identification. Taxonomic status of all specimens at the MUSM has been thoroughly revised and updated (Table S2). Likewise, the corresponding generic name of published species has been accordingly updated (e.g., *Arctocephalus lomasiensis* was replaced by *Hydrarctos lomasensis*) and identifications have been refined (e.g., Monachinae 4 nov. gen. nov. sp. of Muizon and DeVries [1985] was identified as *Australophoca changorum*). Although this study focuses on the late Miocene to the middle Pleistocene vertebrate record (~10-1 Ma), faunas recorded at Chilcatay (~19-17 Ma) and lower Pisco formations between (~14-10 Ma) were also reviewed in order to fully understand evolutionary trends (Table S2).

- ***Temporal clustering of vertebrate data***

Fossiliferous localities have been clustered in four time bins according to their relative chronostratigraphic position, as follows: Miocene older than 10 Ma (> 10 Ma), late Miocene (~10-7 Ma), late Miocene-early Pliocene (~7-4.5 Ma), and late Pliocene-early Pleistocene (2.7-1 Ma). Paleontological data for the Miocene older than 10 Ma (> 10 Ma) time bin was gathered using records from the P0 sequence of the Pisco Formation (e.g., Di Celma et al., 2017; Bosio et al., 2020) and the older Chilcatay Formation (Di Celma et al., 2018; 2019). The fauna from the late Miocene interval (~10-7 Ma) was compiled from records of various localities of the Sacaco sub-basin, including El Jahuay (Alto Grande), Lomas, Aguada de Lomas (levels LM1 to LM12 of Brand et al., 2011; Lambert and Muizon, 2013), Montemar, and Sud-Sacaco west (levels below the unconformity of Muizon and DeVries, 1985). This late Miocene (~10-7 Ma) time bin was also complemented with records from the northern EPB, such as those from Cerro Colorado and Cerro los Quesos (Bianucci et al., 2016a; 2016b; Di Celma et al., 2017). The vertebrate fauna from the late Miocene-early Pliocene (~7-4.5 Ma) time bin comprises taxa from Aguada de Lomas (levels LM13 to LM20 of Brand et al., 2011; Lambert and Muizon, 2013), Sud-Sacaco (localities above the unconformity of Muizon and DeVries, 1985), Sacaco-East, Sacaco Classic, Yauca, Cerro Amarillo, and Acarí. Finally, the late Pliocene-early Pleistocene (2.7-1 Ma) time bin includes the younger Caracoles and Pongo formations. Although the fossiliferous content from the latter formations is still poorly known (Table S2), it has been included as the only way to depict more recent faunal changes. Separation of the Pisco sediments at ~7 My is based on the presence of an unconformity occurring at the westernmost area of the Sud-Sacaco locality (Muizon and DeVries, 1985). Vertebrate taxa exclusively recovered from the Cerro la Bruja (including the CLB level) locality were not considered for coefficient calculations due to its doubtful chronostratigraphic position, which varies from late middle Miocene (~11-10 Ma) according to DeVries and Jud (2018) to late Miocene (9.5-8.9 Ma) according to Di Celma et al., (2017). In the light of the cetacean evidence documented at CLB, the latter age is problematic. This locality records distinct taxa regarded to clades with no representatives within other late Miocene localities of the entire EPB, such as "kentriodontids" (*Belonodelphis*, *Atocetus*) and non-pontoporid iniods (*Brujadelphis*).

- ***Estimates of diversity and extinction-origination per capita rates***

Genus richness and per capita rates of origination (*p*) and extinction (*q*) were calculated for the interval comprised between 11 and 4 Ma to evaluate possible faunal turnover patterns. Genus richness, using per million-year intervals, was assessed using incidence-frequency data by implementing the non-parametric Chao2 index (Chao et al, 2009; Chiu et al., 2014), with a 1000 bootstrap replicates and 95% confidence intervals. The Chao2 was used as richness estimator as it is poorly biased by sample sizes and takes into account rare species and the total number of species observed in the sample to calculate its richness (Chao et al, 2009). Furthermore, per capita rates of origination (*p*) and extinction (*q*) were calculated for the interval comprised between 11 and 4 Ma, using the equations (1) and (2) defined by Foote (2000).

$$p = -\ln(N_{bt}/[N_{bt} + N_b])/\Delta t \qquad (1)$$

$$q = -\ln(N_{bt}/[N_{bt} + N_t])/\Delta t \qquad (2)$$

where N_{bt} is the number of taxa that range through an entire interval, crossing both the top and bottom boundaries, N_b is the number of taxa only crossing the bottom boundary, and N_t the number of taxa only crossing the top boundary. Analyses did not include singletons and used a time bin of one million years ($\Delta t = 1$), so values can be compared to the estimated richness (Chao2 index). In order to avoid border effects, two additional samples (one older than 11 Ma and one younger than 4 Ma) were assembled to include all taxa having extended chronostratigraphic ranges. Statistics analyses were done using R 3.5.0 (R-Core Team, 2013) and the SpadeR package (Chao et al., 2016).

- ***Distribution patterns observed from ~10 to 4.5 Ma***

At first glance, the entire late Miocene-early Pliocene (~10-4.5 Ma; Figs. 6, 7) assemblage is dominated by the same phylogenetic groups and includes similar endemic forms. However, when the stratigraphic distribution of genera is considered, differences in taxonomic richness through time emerge and distinct faunal turnovers by clades are revealed.

- *Cetaceans*. This group was phylogenetically and ecologically diverse throughout the late Miocene-early Pliocene, comprising at least 36 genera (6 mysticetes and 30 odontocetes). Beaked whales (Ziphiidae) are abundant in the late Miocene (~10-7 Ma) beds of the Pisco Formation (Cerro Colorado and Cerro Los Quesos localities), and are mainly represented by stem taxa mostly belonging to the *Messapicetus* clade (Bianucci et al., 2016b). Contrary to the more advanced ziphiids (crown Ziphiidae) that inhabit open ocean areas, the stem forms were mainly coastal dwellers (Bianucci et al., 2016b). Sperm whales (Physeteroidea) are mainly represented by raptorial forms (e.g., *Acrophyseter* and *Livyatan*: Lambert et al., 2010; 2016) and pygmy sperm whales (Kogidae), the latter including *Koristocetus* and the bulky-faced pygmy sperm whale *Scaphokogia* (Muizon, 1988; Collareta et al., 2017; Benites-Palomino et al., 2020).

The fossil record of the physeteroids show no significant changes in their taxonomic composition and diversity throughout this time interval. By contrast, other odontocete clades, such as beaked whales (Ziphiidae), iniod dolphins (Inioidea) and porpoises (Phocoenidae), experienced a turnover at the end of the Tortonian (at ~7 Ma). Prior to this, each of the mentioned clades included three or more genera. However, during the beginning of the Messinian, they suffered a marked decline in their taxonomic diversity with only one representative of each clade recognized throughout this stage (i.e., *Ninozhipius, Pliopontos, Piscolithax*; Muizon, 1984; Lambert et al., 2013). During the ~7- 4.5 Ma interval occurs the first record of a delphinid dolphins, including up to three living genera (*Stenella, cf. Delphinus* and *Cephalorhynchus* and/or *Lagenorhynchus*; Fig., 8; Muizon and DeVries, 1985). The Sacaco locality also yielded the oldest known remains of the extant pygmy sperm whale *Kogia* (MUSM 3888; Benites-Palomino et al., *submitted*) and the first record of a Delphinapterinae from the southern hemisphere (Muizon and DeVries, 1985; Muizon 1988). *Odobenocetops*, a presumably coastal and endemic form from the southeastern Pacific, became common in localities such as Sud-Sacaco, Sacaco and Yauca (Muizon and Domning, 2002). Baleen whale remains, including complete specimens, are abundant from the late Miocene to the early Pliocene; however, their taxonomic diversity is still poorly known as only few of them have been studied (i.e., individuals from LM1 to LM12 in Aguada de Lomas; Brand et al., 2011). Five genera have been documented in rocks between 10 and 7 Ma, but only two genera surpass the Mio-Pliocene transition, the relatively large cetotheriid *Piscocetus*, and the extant rorqual *Balaenoptera* (Bouetel and Muizon, 2006; Pilleri and Siber, 1989). The taxonomy and systematics of *Piscocetus* is uncertain since it has been neither revised nor included in recent phylogenetic analyses.

- *Pinnipeds*. The MUSM collections include various well-preserved earless seals specimens (Phocidae) from late Miocene deposits (at Cerros Los Quesos, Colorado, and La Bruja) from the Ica Valley (Bianucci et al., 2016a; 2016b; Lambert et al., 2017); however, none of them has been properly described and so their taxonomic identity remains uncertain (Lambert et al., 2017). In the Sacaco sub-basin, up to five monachine phocids have been documented (Amson and Muizon, 2013; Muizon, 1981; Muizon and DeVries, 1985). Among them, *Acrophoca longirostris* (Muizon, 1981) is by far the most common taxon along the late Miocene (~10-7 Ma) and late Miocene-early Pliocene (~7-4.5 Ma) time bins, represented by several juvenile and adult individuals. This species, reported from all vertebrate-bearing localities studied herein, shows a much-elongated rostrum towards younger levels. The dwarf monachine *Australophoca* has been reported for the late Miocene (~10-7 Ma) time bin, but it also occurs in the late Miocene-early Pliocene (~7-4.5 Ma). The relatively large-sized but short-snouted taxa, *Piscophoca* and *Hadrokirus*, have only been found in late Miocene-early Pliocene sites (Muizon, 1981; Amson and Muizon, 2013). Current evidence thus suggests the presence of four coeval genera of monachine phocids (i.e., *Acrophoca*, *Piscophoca*, *Hadrokirus*, and *Australophoca*) during the ~7-4.5 Ma interval. A fifth pinniped taxon, recovered from Sacaco, would have also been present (MNHN.F.SAO130).

The last record of phocid seal remains occurs at the early Pliocene (Yauca, ~4.8 Ma; Muizon and DeVries, 1985). No indisputable remains of otariids have been recovered from these Mio-Pliocene levels (Table S2). Recent surveys across the late Pliocene-early Pleistocene deposits of the Caracoles and Pongo formations recovered several specimens referable to the living genus *Arctocephalus* (MUSM 3608, 3628; Table S2; Varas-Malca et al., 2019). The holotype of *Hydrarctos lomasiensis* (MP UNI 04; Museo Mineralógico y Paleontológico de la Universidad Nacional de Ingeniería in Lima, Peru) might have been recovered from similar Plio-Pleistocene beds and originally attributed to the living genus *Arctocephalus* (Muizon, 1978). However, recent phylogenetic studies have considered it either as an early divergent branch of the otariids (Berta and Deméré, 1986; Deméré et al., 2003), or as a taxon closely related to an ancestor of *Arctocephalus*. In any case, this species is key for understanding the phylogenetic relationships and biogeographic history of otariid seals in the southern hemisphere (Berta et al., 2018; Churchill et al., 2014). Lastly, the late Pliocene-early Pleistocene deposits of Caracoles and Pongo formations have also yielded fragmentary bones and teeth of a giant walrus (Odobenidae; Table S2).

- *Sirenians*. The lowermost levels of the Aguada de Lomas locality (~9.5 Ma) yielded the sole remain of a sirenian from the Pisco Formation. It consists of a partial right mandible of a juvenile individual attributed to the dugongid *Nanosiren* (Muizon and Domning, 1985; Domning and Aguilera, 2008). Along with a roughly coeval isolated tooth from the Bahía Inglesa Formation in northern Chile, these are the youngest records of sirenians in the southeastern Pacific (Bianucci et al., 2006; Domning and Aguilera, 2008). A rib from the Sud-Sacaco locality originally referred to a dugongid sirenian because of its extreme compactness (osteosclerosis; Muizon and Domning, 1985; Domning and Aguilera, 2008) in fact pertains to the aquatic sloth *Thalassocnus*, which independently evolved compact bones similar to those of sirenians (Amson et al., 2014). The body mass of *Nanosiren* is calculated in 150 kg and it probably fed upon sea grasses within very shallow waters (Domning and Aguilera, 2008; Velez-Juarbe et al., 2012). Sirenians are obligate aquatic herbivorous and restricted to subtropical and tropical waters (Domning, 2001).

- *Xenarthrans*. This group is represented by *Thalassocnus*, a lineage of marine sloths composed by five species (e.g., Muizon and McDonald, 1995; McDonald and Muizon, 2002; Muizon et al., 2003; 2004a; 2004b), each of them alleged to be found at different horizons (*sensu* Muizon and DeVries, 1985). From older to younger, *Thalassocnus* species and their corresponding locality are: *T. antiquus* (Aguada de Lomas), *T. natans* (Montemar), *T. littoralis* (Sud-Sacaco west), *T. carolomartini* (Sacaco), and *T. yaucensis* (Yauca). *Thalassocnus littoralis* has been also recovered from Aguada de Lomas (LM16), within stratigraphic levels that could be correlated to the Montemar beds (Brand et al., 2011). This taxon is thus documented across the late Miocene (~10-7 Ma) and late Miocene-early Pliocene (~7-4.5 Ma) time bins, being particularly abundant in the latter interval until the uppermost levels (Sacaco, Yauca). Relative to ground sloths, *Thalassocnus* possesses wide and bifurcated transversal processes in the distal caudal vertebrae, a shorter and wider shaft of the radius, and more compact bones (e.g., Muizon and McDonald, 1995; Muizon et al., 2003; Amson et al., 2014). These features are conspicuously enhanced within younger species, and linked to their more aquatic habits (e.g., Muizon et al., 2004b; Amson et al., 2018).

- *Reptiles: Crocodylians and Testudines*. The fossil record of crocodylians includes two extinct long-snouted crocodylian forms, belonging to different clades: *Piscogavialis* (gryposuchine gavialoid; Kraus, 1998; Salas-Gismondi et al., 2019) and a new taxon identified as a Tomistominae (MUSM 161, MUSM 162). *Piscogavialis* was a very large animal, with a skull length of currently known specimens surpassing one meter (SMNK 1282 PAL, type specimen; Kraus, 1998; MUSM 439). Remains of this crocodylian are usually found in anatomical connection, suggesting a rapid burial process. The marine habits of *Piscogavialis* are interpreted based on taphonomy as well as the rostral features regarded by morphometric analyses as typical of marine gavialoids (Salas-Gismondi et al., 2016). The tomistominae crocodylian was probably smaller than *Piscogavialis* at adulthood; the largest skull of this taxon reaches 0.70 m (MUSM 162). These taxa appear to have distinctive chronostratigraphic distributions. Both are recorded from the middle Miocene to the late Miocene (~7 Ma), but only *Piscogavialis* continues up into the early Pliocene (~4.5 Ma; Table S2). At present, no crocodylian species occur in the Peruvian Pacific coast south of ~4.1ºS. As for testudines, remains of marine turtles have only been recovered from the Ica Valley. The record consists of the chelonid *Pacifichelys urbinai* (Parham and Pyenson, 2010; Bianucci et al., 2016b) and one dermochelyid species (MUSM 407) more closely related to *Dermochelys* than to *Psephophorus*.

- *Aves.* Coastal seabirds, such as boobies (Sulidae), cormorants and penguins (Phalacrocoracidae) and penguins (Spheniscidae), are relatively well-documented in the fossil record of the Pisco Formation by several skeletons and hundreds of isolated bones (Muizon and DeVries, 1985; Cheneval, 1993; Stucchi, 2002; 2008; Stucchi and DeVries, 2003; Stucchi et al., 2003; 2015b; Urbina and Stucchi, 2005; Acosta-Hospitaleche et al., 2011). In contrast, remains of pelicans are restricted to a single bone occurrence from the Montemar locality in the Sacaco sub-basin (Altamirano-Sierra, 2013). The fossil record from the Pisco Formation also includes specimens of extinct taxa of cathartiforms (New World vultures; Stucchi and Emslie, 2005; Stucchi et al., 2015a), procellariforms (e.g., petrels, albatrosses), charadriiforms and other seabirds with no extant close relatives, such as pelagornithids and the sulid *Ramphastosula* (Stucchi and Urbina, 2004; Chavez et al., 2007; Stucchi, 2008; Stucchi et al., 2015b).

- *Chondrichthyes*. The modern Peruvian chondrichtyans (sharks, rays, skates and chimaeras) or cartilaginous fishes comprises 66 species of sharks and 43 of rays, all of them within 11 clades (Cornejo et al., 2015). Nine of these (Lamniformes, Heterodontiformes, Carcharhiniformes, Rhinopristiformes, Hexanchiformes, Pristiophoriformes, Squatiniformes, Myliobatiformes, and Chimaeriformes) are represented in the fossil record of the Pisco Formation (Muizon and DeVries, 1985; Landini et al., 2017; undescribed MUSM specimens). The record is mostly dominated by Carcharhiniformes and Lamniformes, from which up to seven different genera have been recognized within each clade (Table S2). Teeth of the requiem sharks belonging to *Carcharhinus* and the lamnid *Cosmopolitodus* (=*Carcharodon*) are relatively common, in contrast to those of the lemon shark *Negaprion* and the sawshark *Pristiophorus*, which are represented by a few isolated pieces. The non-serrated teeth of *Cosmopolitodus hastalis* are recorded throughout the late Miocene (~10-7 Ma) time bin, while teeth with incipient serrations appear in the record for the first time in Montemar and Sud-Sacaco-west localities (~7 Ma; *Carcharodon hubbelli* type of teeth). Serrated teeth typically of *Carcharodon* are reported within the late Miocene-early Pliocene (~7-4.5 Ma; Ehret et al., 2012) and the late Pliocene-early Pleistocene (2.7-1 Ma) time bins (Table S2). Several shark taxa today inhabiting the southeastern Pacific have a continuous fossil record in the Pisco Formation (that in some groups goes back to the Chilcatay Formation; Bianucci et al., 2016a; 2016b; Landini et al., 2019). This is, for instance, the case of the short fin Mako shark (*Isurus oxyrinchus*), the hammerhead shark (*Sphyrna*), the copper shark (*Carcharhinus brachyrurus*), and the bull shark (*Carcharinus leucas*). The otodontid lamniforms, a popular clade known as 'megatooth' sharks, are all extinct and comprise large to giant sharks recovered from the Chilcatay and Pisco formations (Table S2). The giant *Carcharocles megalodon* was the last survivor of this group and has been recorded up to the top of the Pisco deposits (Bianucci et al., 2016a; 2016b; Muizon and DeVries, 1985; Landini et al., 2017). To date, *Carcharocles* is absent from Plio-Pleistocene deposits of the EPB (Caracoles and Pongo formations). The extant lamnids *Carcharodon*, *Carcharias* and *Pseudocarcharias* are found as fossils in the Pisco Formation (Table S2) but no longer inhabit the Peruvian coasts. The broadnose sevengill shark *Notorhynchus* is the only shark from the Caracoles Formation not found in older deposits. Myliobatiformes and Chimaeriformes are restricted to *Myliobatis* and *Callorhinchus*, respectively.

- *Non-aquatic mammals*. Non-aquatic vertebrate remains are rare in the Pisco Formation beds, yet they constitute the only evidence about the Neogene terrestrial fauna of the area known so far (Table S2). The published record includes postcranial elements of the carnivoran procyonid *Cyonasua* (MNHN SAS 1625, MNHN PPI 262; Muizon and DeVries, 1985; Tarquini et al., 2020). The unpublished record encompasses a mandibular fragment of the hystricognath rodent *Tetrastylus* (MNHN PPI 263, 264), a portion of a fused radius-ulna and trochlear humerus of a medium-sized macraucheniid litoptern (MUSM 226) and a calcaneus of a small marsupial (MUSM 225). These remains were all recovered from localities clustered in the late Miocene (~10-7 Ma) time bin, such as Montemar, Aguda de Lomas, and Lomas, the latter argued to be slightly older (Brand et al., 2011). The youngest record corresponds to an isolated femur of *Cyonasua* (MNHN PPI 262) recovered in Sud-Sacaco, at about the Tortonian/Messinian boundary (Tarquini et al., 2020).

Supplementary Table 1. Existing chronostratigraphic data from the East Pisco Basin, including age constraints based on radiometric, isotopic and (bio)stratigraphic information.

Reference	Dating Method		Coordinates		Observations	Ica Valley					Sacaco Sub-basin					
			Lat	Long		Cerro la Bruja	Los Quesos	Cerro Colorado	Cerro Ballena	Other localities	EL Jahuay	Aguada de Lomas	Montemar	Sud-Sacaco	Sacaco	Other localities
Muizon and Bellon, 1980	Radiometric	K-Ar in biotite - ash	Not given												3.9 +- 0.2 Ma	
Muizon and DeVries, 1985	Radiometric	K-Ar in biotite - ash	Not given			~13-11 Ma						8 - 8.8 Ma				
Muizon and Bellon, 1986	Radiometric	K-Ar in biotite - ash	Not given								9.38+- 0.47 Ma / 9.63 +- 0.48	7.93+-0.4 Ma / 8.04 +-0.40 Ma / 8.85 +- 0.66 Ma				
Dunbar et al., 1990 palaeo3	Radiometric	K-Ar in biotite - ash	13°38' s	76°11'W						Monte Caucato section 6.89 +- 0.10 Ma						
Dunbar et al., 1990 palaeo3	Radiometric	K-Ar in biotite - ash	14°26's	75°46'W						Queso Grande section: 6.75 + 0.18 Ma						
Dunbar et al., 1990 palaeo3	Radiometric	K-Ar in biotite - ash	14°56'S	75°15'W						Molde de Queso: 5.49 +- 0.12 Ma						
Dunbar et al., 1990 palaeo3	Radiometric	K-Ar in biotite - ash	14°56'S	75°16'W						Huaracangana : 6.42 +-0.12 Ma						
DeVries, 1998	Radiometric	Ar–Ar ash	14°37'31 S	75°38'12 W	(locality 87DV 494-2 Snee)					9.20 Ma Ica River Valley						
DeVries, 1998	Radiometric	Ar–Ar ash	14°37'31 S	75°38'12 W	(locality 87DV 484-3B Snee)					YESERA (YES) 9.22 Ma						
Ehret et al., 2012 - Palaeontology	Isotopic	87Sr / 86Sr in 3 mollusk shells	Not given		*MTM includes localities at SAS below the uncomformity of Muizon & DeVries, 1985 (i.e. SAS oeste or "segunda poza")						7.46 Ma (9.03–6.51)		7.30 Ma (8.70–6.45)	6.59 Ma (10.77–2.50) / 5.93 Ma (6.35–5.47)	5.89 Ma (6.76–4.86)	
Reinterpreted data from Ehret et al., 2012, using McArthur et al., 2012 (Fitness V.5)											7.35 Ma (8.550–6.50)		7.15 Ma (8.25–6.52)	6.55 Ma (7.2–6.1) / 5.9 Ma (6.25–5.52)	5.76 Ma (6.2–5.45)	
unpublished report in Ehret et al., 2012	Radiometric	Ar–Ar ash	Not given		locality DV 514-2 Snee										5.75 Ma ± 0.05	
This study	Biostratigraphic		Multiple sites													SACACO ESTE SAO-E: ~5.5 Ma / ~6-5.8 Ma
Brand et al., 2011	Radiometric	Ar/Ar on biotite	Not given		Reinterpreted data from Muizon and Bellon, 1986	9.2 Ma (50 m above CLB level; between m4 y m5) / 10 - 7.5 Ma			6.96 - 6.85 Ma Between M16 y M17: A03-139C)							
O`Hare, 2015	Radiometric	Ar–Ar ash	14°31'42 S	75°34'43 W						YESERA: 7.12 + 0.09 Ma (A07-27B)						

Reference	Dating Method		Coordinates		Observations	Ica Valley					Sacaco Sub-basin					
			Lat	Long		Cerro la Bruja	Los Quesos	Cerro Colorado	Cerro Ballena	Other localities	EL Jahuay	Aguada de Lomas	Montemar	Sud-Sacaco	Sacaco	Other localities
O`Hare, 2015	Radiometric	Ar–Ar ash	14°23'53 S / 14°23'43 S	75°42'04 W / 75°42'05 W						CERRO BLANCO: 6.82+- 0.07 Ma (A07-36A) / 6.75+-0.13 Ma (A07-35E)						
O`Hare, 2015	Radiometric	Ar–Ar ash	14°21'45 S / 14°20'45 S	75°42'42 W / 75°43'06 W					6.87+- 0.04 Ma (A03-139C) / 6.43+- 0.12 Ma (A07-77A)							
Lambert and Muizon 2013 - JVP	Stratigraphic		Not given		Reinterpreted data from Muizon and Bellon, 1986						9.38 - 9.63 Ma	7.93 - 8.04 Ma (between M6 & M7) / 8.85 Ma (between M5 & M6)				
unpublished report in Esperante et al., 2015 (Kevin Nick, written comm)	Radiometric	Ar–Ar in biotite	Not given							CERRO BLANCO: 6.82 - 6.07 Ma						
unpublished report in Esperante et al., 2015 (Kevin Nick, written comm)	Radiometric	Ar–Ar in biotite	Not given				7.73 - 7.11 Ma		6.94 - 6.43 Ma	Hueco la Zorra (HLZ) 6.78 - 6.16 Ma						
Di Celma et al., 2016 Journal of Maps	Radiometric	Ar–Ar in biotite					6.93-6.71 Ma (above P2-6 [flor])									
Di Celma et al., 2016 Journal of Maps	Biostratigraphic	Diatoms - FO of *Thalassiosira antiqua*			Bruja Level	8.5 Ma (Bruja Level) / ~9.9 - 8.9 Ma	7.35 -7.1 Ma (end of Member E and base of Member F = above estrella level and below flor level)									
Di Celma et al., 2016 Journal of Maps	Radiometric	40Ar/39Ar in biotite	14°30'50 S	75°43'07 W	highest tephra from stratigraphic section		t > 6.71 ± 0.02 Ma (CLQ-T9b)									
Di Celma et al., 2016 Journal of Maps	Radiometric	40Ar/39Ar in biotite	14°30'50 S	75°43'01 W	Mono marker bed		6.93 ± 0.09 Ma (CLQ-T1)									
Di Celma et al., 2016 Journal of Maps	Radiometric	40Ar/39Ar in biotite	14°30'50 S	75°43'06.8 W	Three dated ash layers on top of the Ballena marker bed		7.55 ± 0.05 Ma (top of Ballena marker bed; CLQ-T49)									
Barron, 2003	Biostratigraphic							~9.9-8.9 Ma								
Gariboldi et al., 2017 Newsl. Stratig	Radiometric	40Ar/39Ar in biotite					7.55 Ma; 6.93 Ma; 6.71 Ma	9.10 Ma (Lower Allomemb, 30 mabs)								
Di Celma et al., 2017 (Rev.Itali.Paleo)	Stratigraphic					7.55 Ma (below P2-5 [below condor level])										
Di Celma et al., 2017 (Rev.Itali.Paleo)	Radiometric	Ar–Ar ash	14°35'40.2 S	75°40'04.8 W						Chilcatay Fm Top 17.99 Ma						
Di Celma et al., 2018, 2019	Radiometric									Chilcatay Fm 19.25-18.02 Ma						

Reference	Dating Method		Coordinates		Observations	Ica Valley					Sacaco Sub-basin					
			Lat	Long		Cerro la Bruja	Los Quesos	Cerro Colorado	Cerro Ballena	Other localities	EL Jahuay	Aguada de Lomas	Montemar	Sud-Sacaco	Sacaco	Other localities
Di Celma et al., 2017 (Rev.Itali.Paleo)	Stratigraphic									P0: 17.99 ± 0.10 to 9.00 ± 0.02 Ma						
Marx et al., 2017; DiCelma et al., 2018	Biostratigraphic									P0: ~13.8-11.6; ~11.7-10 Ma						
Di Celma et al., 2017 (Rev.Itali.Paleo)	Radiometric	Ar–Ar ash	14°34'15.8 S	75°43'44.2 W						9.00 ± 0.02 Ma Cerro Cadenas de los Zanjones						
Di Celma et al., 2017 (Rev.Itali.Paleo)	Stratigraphic							P1: 9.10 ± 0.04 Ma		P1: 9.5 to 8.9 Ma						
Di Celma et al., 2017 (Rev.Itali.Paleo)	Radiometric	40Ar/39Ar in biotite	14°34'29 S	75°39'53.7 W		CLB: 7.45 ± 0.01 Ma (LB-T11 174 abs)										
Di Celma et al., 2017 (Rev.Itali.Paleo)	Stratigraphic									P2: 8.5 Ma - older than 6.71 ± 0.02 Ma						
Bosio et al., 2019 (NoS)	Radiometric	Ar–Ar ash	Multiple sites northern EPB (Ica Valley)							P1: 9.5 to 8.6 Ma						
Bosio et al., 2019 (NoS)	Radiometric	Ar–Ar ash	Multiple sites northern EPB (Ica Valley)							P2: 8.4 Ma - older than 6.71 ± 0.02 Ma						
Bosio et al., 2020 (JSAMES)	Isotopic	87Sr / 86Sr in different type of samples	Multiple sites northern EPB (Ica Valley)							Lower P0: 13.45 Ma (12.45-14.80 Ma)						
Marx et al., 2017	Biostratigraphic									SANTA ROSA SRA: ~13.8-11.6 Ma						
Di Celma et al., 2017 (Rev.Itali.Paleo)	Biostratigraphic									MALPASO MLP: ~17.9-10 Ma						
Unpublished data (DeVries and Ochoa)	Biostratigraphic		Multiple sites northern EPB (Ica Valley)							LABERINTO LAB-Sula site: 14-12 Ma						
Unpublished data, MUSM	Biostratigraphic				Presence of 'archaic' Acrophoca, MUSM					CORREVIENTO CVT: ~8 - 7 Ma						
Stucchi et al., 2015a	Stratigraphic				Age based on correlation with ELJ					LAGUNA SECA LAG: ~10-8.8 Ma; ~9.5 Ma						
Brand et al., 2011	Stratigraphic															LOMAS LMS: ~10.5-9 Ma
This study	Biostratigraphic				faunal correlation with Yauca (YAU)											ACARI ACR: ~4.8 Ma

Supplementary Table 2. Compiled paleontological data used in this review, listed as genus per locality. Table also includes genera from the modern pooled sample used as a benchmark for comparing fossil to modern coastal-marine vertebrate faunas

Genus Code	Present at Sacaco sub-basin	Taxa (Genus)	Phylogenetic group			Time Bin					Reference
						>10 Ma	10-7 Ma	7-4.5 Ma	2.7-~1 Ma	Modern	
1		*Tiucetus*	Cetacea	Mysticeti		SRA					Marx et al., 2017
2	x	*Miocaperea*					AGL				Bisconti, 2012
3	x	*Piscobalaena*					AGL MTM	SAS CBA			Pilleri & Siber 1989; Bouetel & Muizon 2006; Marx et al., 2017
4	x	*Piscocetus*						SAO			Pilleri & Pilleri, 1989
5	x	*Incakujira*					AGL				Marx & Kohno, 2016
6	x	*Balaenoptera*					AGL MTM	SAS SAO	CAR	X	Pilleri & Pilleri, 1989; MUSM; ACOREMA, 2018***
7		*Eubalaena*								X	ACOREMA, 2018***
8		*Megaptera*								X	ACOREMA, 2018***
9		*Inticetus*		Odontoceti		CHIL					Lambert et al., 2017; MUSM 1980
10		*Huaridelphis*				CHIL					Lambert et al., 2014; MUSM 1396; MUSM 1403
11		*Chilcacetus*				CHIL					Lambert et al., 2015; MNHN.F.PRU11; MUSM 1401,
12		*Notocetus*				CHIL					Bianucci et al., 2015;2020; MUSM 1395; MUSM 3896; MUSM 3897
13		*Furcacetus*				CHIL					Bianucci et al., 2020; MUSM 487
14		*Ensicetus*				CHIL					Bianucci et al., 2020; MUSM 3898
15		*Macrosqualodelphis*				CHIL					Bianucci et al., 2018; MUSM 2545
16		Platanidelphidi				CHIL					Bianucci et al. 2020; MUSM 3899
17		Physeteroidea 1				P0					MUSM
18		Physeteroidea 2				P0					MUSM
19		Physeteroidea 3				CHIL					MUSM
20		*Livyatan*			Physeteroidea		CCO				Lambert et al., 2010
21	x	*Acrophyseter*					CCO CLB AGL CLQ M	SAS			Lambert et al., 2009; 2017
22	x	*Scaphokogia*					AGL MTM	SAS			Muizon 1988; Benites-Palomino et al., 2020
23		*Platyscaphokogia*					CLQ CLB				Collareta et al., in prep., MUSM
24	x	*Koristocetus*					AGL (LM16)	SAO			Collareta et al., 2017
25	x	*Kogia*						SAO		X	ACOREMA, 2018***, MUSM 3888
26		*Physeter*								X	ACOREMA, 2018***
27		*Chimuziphius*			Ziphiidae		CCO				Bianucci et al., 2016a
28		*Messapicetus*					CCO CLQ				Bianucci et al., 2010, 2016a
29		*Chavinziphius*					CLQ				Bianucci et al., 2016a
30		*Nazcacetus*					CLQ				Lambert et al., 2009
31	x	*Ninoziphius*					AGL	SAS			Muizon 1984; Muizon & DeVries, 1985; MUSM
32		*Mesoplodon*								X	ACOREMA, 2018***
33		*Ziphius*								X	ACOREMA, 2018***
34		*Incacetus*			Inioidea	SRO					Colbert, 1944; Muizon, 1988
35		*Belonodelphis*				CLB?	CLB?				Muizon, 1988
36		*Brujadelphis*				CLB?	CLB?				Lambert et al., 2017; MUSM 1400
37		*Atocetus*				CLB?	CLB?				Muizon, 1988
38	x	*Brachydelphis*				CLB?	CLB? CCO, CVT, ELJ	AGL, HLZ			Muizon & DeVries, 1985; Muizon 1988; Gutstein et al. 2009; Lambert & Muizon, 2013; periotic identified by Bianucci at HLZ
39		*Samaydelphis*				CLB?	CLB? CCO CLQ, HLZ				Lambert et al., 2020; MUSM 566; MUSM 565; MUSM 2541; MUSM 3903
40	x	*Pliopontos*					MTM	SAS			Muizon, 1984, 1988; Muizon & DeVries, 1985
41	x	*Odobenoceptos*					MTM, HLZ	SAS SAO YAU			Muizon, 1993; Muizon and Domning 2002; MUSM
42	x	Delphinapterinae						SAO			Muizon & DeVries, 1985
43	x	*Australithax*			Phocoenidae		ELJ				Muizon, 1988
44	x	*Lomacetus*					AGL				Muizon, 1988
45	x	*Piscolithax*					AGL MTM	SAS SAO			Muizon & DeVries, 1985
46		*Phocoena*								X	ACOREMA, 2018***
47	x	*Hemisyntrachelus*			Delphinidae			SAS SAO			Muizon, 1984; Pilleri & Pilleri, 1989
48	x	*Delphinus*						SAO		X	Muizon & DeVries, 1985
49	x	Delphininae							O CAR	?	MUSM
50	x	*Stenella*						SAO	CAR	X	Muizon & DeVries, 1985; MUSM
51		*Feresa*								X	ACOREMA, 2018***
52		*Globicephala*								X	ACOREMA, 2018***
53		*Grampus*								X	ACOREMA, 2018***
54		*Lagenorhynchus*								X	ACOREMA, 2018***
55	x	Lissodelphininae						O SAO			MNHN
56		*Lissodelphis*								X	ACOREMA, 2018***
57		*Orcinus*								X	ACOREMA, 2018***
58		*Peponocephala*								X	ACOREMA, 2018***
59		*Pseudorca*								X	ACOREMA, 2018***
60		*Steno*								X	ACOREMA, 2018***
61		*Tursiops*								X	ACOREMA, 2018***

Genus Code	Present at Sacaco sub-basin	Taxa (Genus)	Phylogenetic group		Time Bin >10 Ma	10-7 Ma	7-4.5 Ma	2.7-~1 Ma	Modern	Reference
62	x	*Acrophoca*	Pinnipeds	Phocidae		ELJ AGL MTM	SAS SAO			Muizon 1984; Muizon & DeVries, 1985; MUSM
63	x	*Australophoca*				ELJ AGL MTM	SAS SAO			Valenzuela-Toro et al., 2015; MNHN
64	x	*Piscophoca*					SAS SAO			Muizon, 1984
65	x	*Hadrokirus*					SAS			Amson & Muizon, 2013
66		Monachinae 1			CLB?	CLB?				MNHN
67		Monachinae 2			CLB?	CLB?				MNHN, MUSM
68	x	Monachinae 3					SAO			MNHN
69	x	*Hydrarctos*		Otariidae				CAR?		Muizon, 1978; MUSM
70	x	*Arctocephalus*						CAR	X	ACOREMA, 2018***; MUSM 3608; MUSM 3628
71		*Otaria*							X	ACOREMA, 2018***
72	x	Odobenidae						CAR PON		MUSM
73	x	*Nanosiren*	Dugongidae			AGL				Domming & Aguilera, 2008
74	x	*Thalassocnus*	Megatheriidae			AGL MTM	SAS SAO SAO-E ACR YAU			Muizon & McDonald, 1995; McDonald & Muizon, 2002; Muizon et al., 2003, 2004a, 2004b, Amson et al., 2014a, 2014b,2015, 2018
75	x	*Tetrastylus*	Non-aquatic mammals			AGL				MUSM
76	x	*Cyonasua*				MTM	SAS			Tarquini et al., 2019; Tarquini et al., submitted
77	x	Macraucheniidae				LMS				MUSM
78	x	Marsupialia				LMS				MUSM
79		*Lontra*	Mustelidae						X	ACOREMA, 2018***
80	x	*Piscogavialis*	Crocodylians		LAB P0	ELJ AGL MTM	SAS SAO SAO-E YAU			Kraus, 1997; Salas-Gismondi et al., 2016, LAB age from Ochoa and DeVries unpublished data
81	x	Tomistominae			CHIL, PAR	CCO CVT AGL MTM				DeVries 2002; Salas, 2003
82		*Pacifichelys*	Testudines			CCO				Parham & Pyenson, 2010
83		*Chelonia*							X	Kelez et al., 2005 +
84		*Lepidochelys*							X	Kelez et al., 2005 +
85		*Caretta*							X	Kelez et al., 2005 +
86		*Eretmochelys*							X	Kelez et al., 2005 +
87		*Natemys*			CHIL					Wood et al., 1996
88		*Dermochelys*				CVT			X	MUSM
89	x	*Pelagornis*	Seabirds		MPS	ELJ LMS AGL	SAS SAO			Cheneval, 1993; Stucchi, 2008; Chavez et al., 2007; MUSM
90	x	*Perugyps*		CATHARTIFORMES		MTM				Stucchi & Emslie, 2005
91		*Kuntur*				LAG				Stucchi et al., 2015b
92		*Coragyps*							X	BirdLife International, 2020
93		*Cathartes*							X	BirdLife International, 2020
94	x	*Ramphastosula*					SAS			Stucchi & Urbina, 2004; Stucchi et al., 2016
95	x	*Morus*				MTM				Stucchi 2003
96	x	*Sula*			LAB	CCO ELJ AGL MTM	SAS SAO	CAR	X	Cheneval, 1993; Stucchi 2003
97	x	*Phalacrocorax*				AGL MTM	SAS SAO	PON	X	Cheneval, 1993; Urbina & Stucchi, 2005
98		*Palaeospheniscus*			CHIL					Acosta-Hospitaleche & Stucchi, 2011
99	x	*Spheniscus*				CLB ELJ AGL MTM	SAO-E SAO	CAR PON	X	Cheneval, 1993; Göhlich, 2007; Stucchi et al, 2003; Stucchi, 2002; Stucchi, 2007
100	x	Puffinini				O ELJ AGL, MTM	O SAS SAO	O CAR PON	?	Stucchi & Urbina, 2004
101		*Larosterna*							X	BirdLife International, 2020
102		*Larus*							X	BirdLife International, 2020
103	x	*Fulmarus*					SAS SAO		Offshore (openwaters)	Cheneval, 1993; MUSM
104		*Oceanodroma*							X	BirdLife International, 2020
105		*Pelecanoides*							X	BirdLife International, 2020
106	x	*Pelecanus*				MTM			X	Altamirano-Sierra, 2013; BirdLife International, 2020
107		*Sterna*							X	BirdLife International, 2020
108		*Thalassarche*							X	BirdLife International, 2020
109	x	*Carcharocles*	Chondondrichthyes		CHIL P0	CCO CLB CLQ ELJ A(	SAS SAO			Landini et al., 2019
110	x	*Cosmopolitodus*			CHIL P0	CLB CCO CLQ ELJ AGL MTM				Landini et al., 2019; Bosio et al., 2020
111	x	*Carcharodon*					SAS SAO SAO-E YA(	CAR PON		Cornejo et al., 2015
112	x	*Isurus*			CHIL P0	ELJ AGL MTM	SAS SAO SAO-E YA(	CAR PON	X	Muizon & DeVries, 1985; MUSM; Altamirano, 2014^; Bosio et al., 2020
113		*Anotodus*			CHIL	CCO				Landini et al., 2017; 2019
114		*Carcharoides*				CCO				Landini et al., 2017
115	x	*Carcharias*			CHIL	CCO CLQ	SAS SAO			Landini et al., 2017; 2019
116		*Pseudocarcharias*				CCO				Landini et al., 2017
117	x	*Alopias*			CHIL	CCO CLQ	SAS SAO	CAR PON	X	Landini et al., 2017; 2019
118		*Physogaleus*			CHIL	CCO				Landini et al., 2017; 2019
119		*Negaprion***			CHIL	CCO			X	Landini et al., 2017; 2019
120	x	*Heterodontus*				ELJ	SAS, SAO-E		X	MUSM
121	x	*Hexanchus*				ELJ AGL MTM	SAO		X	Muizon & DeVries, 1985
122		*Hemipristis***			CHIL P0	CLB				Landini et al., 2019; Bosio et al., 2020
123	x	*Pristiophorus***				ELJ				Muizon & DeVries, 1985
124	x	*Callorhinchus*					SAO		X	Muizon & DeVries, 1985

Genus Code	Present at Sacaco sub-basin	Taxa (Genus)	Phylogenetic group	Time Bin					Reference
				>10 Ma	10-7 Ma	7-4.5 Ma	2.7-~1 Ma	Modern	
125	x	*Carcharhinus*	Chondondrichthyes	CHIL P0	ELJ AGL	SAS SAO SAO-E YAU	CAR	X	Landini et al., 2017; Bosio et al., 2020
126	x	*Galeorhinus*				SAS SAO-E	CAR	X	Muizon & DeVries, 1985
127		*Galeocerdo*		CHIL P0	CCO			X	Landini et al., 2017; 2019; Bosio et al., 2020
128		*Anoxypristis***		P0					Bosio et al., 2020
129	x	*Squatina*		CHIL	CCO	SAS SAO-E		X	Landini et al., 2017; 2019; Altamirano, 2014^
130		*Mustelus*						X	Cornejo et al., 2015; Altamirano, 2014^
131	x	*Notorynchus*					CAR	X	MUSM; Altamirano, 2014^
132		*Prionace*						X	Cornejo et al., 2015;
133		*Schroederichthys*						X	Altamirano, 2014^ Cornejo et al., 2015
134	x	*Sphyrna*		CHIL	CCO	SAS SAO		X	Landini et al., 2017; 2019; Altamirano, 2014^
135		*Triakis*						X	Cornejo et al., 2015; Altamirano, 2014^
136	x	*Myliobatis*		CHIL P0	CCO CLQ AGL MTM	SAS SAO SAO-E YAU	CAR	X	Landini et al., 2017
137		*Dasyatis*						X	Cornejo et al., 2015

> 10 Ma	
Chilcatay Fm localities	CHIL
Pisco 0	P-0
Santa Rosa	SRA
Malpaso	MPS
Laberinto-Sula site	LAB
Cerro La Bruja	CLB
10.0-7.0 Ma	
Cerro Colorado	CCO
Cerro Los Quesos	CLQ
Correviento	CVT
Laguna Seca	LAG
El Jahuay	ELJ
Aguada de Lomas	AGL
Montemar	MTM*
Hueco La Zorra	HLZ
Lomas	LMS
7.0-4.5 Ma	
Cerro Ballena	CBA
Sacaco Sur	SAS
Sacaco	SAO
Sacaco Este	SAO-E
Yauca	YAU
Acari	ACR
2.7-1.5 Ma	
Caracoles Fm	CAR
Pongo Fm	PON

Note that all abbreviations listed before are referring to localities and not to vertebrate-bearing levels (as originally indicated by Muizon & DeVries, 1985).

O unclear whether a genus from the fossil record corresponds with a living one

*MTM includes localities at SAS below the uncomformity of Muizon & DeVries, 1985 (i.e. SAS oeste or "segunda poza")
** Modern genus, no inhabiting within the Humboltd System
*** ACOREMA, 2018; http://www.acorema.org.pe/documentos/Lista_de_mamiferos_marinos_de_la_provincia_de_Pisco_2018.pdf
+ Kelez et al., 2005; https://www.cms.int/sites/default/files/publication/Tortugas_Peru_informe_final_CMS_En.pdf
^ Altamirano, 2014 http://www.acorema.org.pe/documentos/Los_Tiburones_de_la_Provincia_de_Pisco-ACOREMA-2014.pdf

Supplementary Table 3. LA-MC-ICP-MS data and U/Pb calculated weighted mean ages for collected ash samples.

- **Sample: MG3-25 (Locality: Sacaco Classic [Chacra Area]**

Crystal ID	Isotopic ratios														Estimated Ages								
	$^{207}Pb/^{235}U$*	± 1σ	$^{206}Pb/^{238}U$	± 1σ	$^{207}Pb/^{206}Pb$	± 1σ	$^{207}Pb/^{235}U$	± 2σ	$^{206}Pb/^{238}U$	± 2σ	Rho	$^{207}Pb/^{206}Pb$	± 2σ	$^{207}Pb/^{235}U$ (Ma)	± 2σ	$^{206}Pb/^{238}U$ (Ma)	± 2σ	$^{207}Pb/^{206}Pb$ (Ma)	± 2σ	% Discordance	Best age (Ma)	± 2σ
MG3-25_4	0.00485	0.00007	0.00070	0.00000	0.04743	0.00056	0.00556	2.7	0.00086	1.1	0.39	0.04690	2.5	5.6	0.2	5.5	0.1	44.0	58.9	1.6	**5.541**	**0.059**
MG3-25_8	0.00492	0.00006	0.00071	0.00000	0.04678	0.00050	0.00554	2.5	0.00087	1.1	0.43	0.04626	2.3	5.6	0.1	5.6	0.1	11.0	54.2	0.2	**5.595**	**0.060**
MG3-25_38	0.00528	0.00008	0.00072	0.00000	0.04971	0.00051	0.00596	2.4	0.00088	1.0	0.42	0.04916	2.2	6.0	0.1	5.7	0.1	155.0	50.8	6.1	**5.670**	**0.056**
MG3-25_29	0.00497	0.00005	0.00072	0.00000	0.04829	0.00034	0.00580	1.9	0.00088	1.1	0.56	0.04775	1.6	5.9	0.1	5.7	0.1	86.5	37.4	3.3	**5.678**	**0.060**
MG3-25_37	0.00520	0.00017	0.00072	0.00000	0.04972	0.00100	0.00599	4.2	0.00088	1.1	0.27	0.04917	4.1	6.1	0.3	5.7	0.1	155.5	95.6	6.1	**5.692**	**0.065**
MG3-25_6	0.00606	0.00018	0.00072	0.00000	0.05508	0.00110	0.00664	4.2	0.00088	1.2	0.29	0.05446	4.1	6.7	0.3	5.7	0.1	390.0	91.0	15.2	**5.694**	**0.071**
MG3-25_3	0.00601	0.00012	0.00072	0.00000	0.05658	0.00078	0.00683	3.1	0.00089	1.2	0.39	0.05595	2.8	6.9	0.2	5.7	0.1	450.0	63.2	17.5	**5.704**	**0.068**
MG3-25_7	0.00496	0.00009	0.00072	0.00000	0.04753	0.00069	0.00574	3.2	0.00089	1.2	0.37	0.04700	3.0	5.8	0.2	5.7	0.1	49.0	71.4	1.8	**5.710**	**0.067**
MG3-25_23	0.00574	0.00013	0.00072	0.00000	0.05203	0.00069	0.00629	3.0	0.00089	1.2	0.40	0.05145	2.7	6.4	0.2	5.7	0.1	260.5	63.1	10.3	**5.713**	**0.068**
MG3-25_30	0.00616	0.00016	0.00073	0.00000	0.05218	0.00095	0.00633	3.9	0.00089	1.1	0.29	0.05160	3.7	6.4	0.2	5.7	0.1	267.5	85.1	10.5	**5.732**	**0.064**
MG3-25_35	0.00657	0.00023	0.00073	0.00000	0.05019	0.00094	0.00610	4.0	0.00089	1.2	0.30	0.04963	3.8	6.2	0.2	5.7	0.1	177.0	88.9	7.0	**5.741**	**0.068**
MG3-25_10	0.00544	0.00015	0.00073	0.00000	0.04981	0.00110	0.00605	4.6	0.00089	1.2	0.25	0.04926	4.5	6.1	0.3	5.7	0.1	159.5	104.7	6.3	**5.741**	**0.067**
MG3-25_19	0.00567	0.00013	0.00073	0.00000	0.05137	0.00098	0.00624	4.0	0.00089	1.0	0.26	0.05080	3.9	6.3	0.3	5.7	0.1	231.5	89.6	9.1	**5.743**	**0.060**
MG3-25_16	0.00585	0.00016	0.00073	0.00000	0.05361	0.00130	0.00653	5.0	0.00089	1.1	0.21	0.05301	4.9	6.6	0.3	5.8	0.1	329.0	111.2	12.9	**5.754**	**0.062**
MG3-25_15	0.00563	0.00010	0.00073	0.00000	0.05050	0.00063	0.00615	2.8	0.00089	1.1	0.39	0.04993	2.6	6.2	0.2	5.8	0.1	191.5	60.3	7.5	**5.759**	**0.063**
MG3-25_36	0.00517	0.00012	0.00073	0.00000	0.05308	0.00090	0.00648	3.6	0.00089	1.1	0.31	0.05249	3.5	6.6	0.2	5.8	0.1	306.5	78.9	12.0	**5.767**	**0.065**
MG3-25_20	0.00726	0.00034	0.00073	0.00000	0.06922	0.00280	0.00845	8.2	0.00090	1.4	0.17	0.06845	8.1	8.5	0.7	5.8	0.1	882.0	168.0	32.5	**5.768**	**0.081**
MG3-25_40	0.00568	0.00015	0.00073	0.00000	0.05163	0.00089	0.00633	3.7	0.00090	1.2	0.31	0.05105	3.5	6.4	0.2	5.8	0.1	243.0	81.1	9.6	**5.799**	**0.068**
MG3-25_28	0.00739	0.00036	0.00074	0.00000	0.05215	0.00120	0.00642	4.8	0.00090	1.2	0.24	0.05157	4.7	6.5	0.3	5.8	0.1	266.0	106.8	10.5	**5.814**	**0.068**
MG3-25_18	0.00554	0.00011	0.00074	0.00000	0.04979	0.00061	0.00617	2.8	0.00091	1.1	0.38	0.04923	2.6	6.2	0.2	5.9	0.1	158.5	59.7	6.2	**5.856**	**0.061**
MG3-25_11	0.00859	0.00024	0.00074	0.00000	0.07436	0.00170	0.00922	4.8	0.00091	1.1	0.24	0.07353	4.6	9.3	0.4	5.9	0.1	1028.5	93.5	37.1	**5.860**	**0.067**
MG3-25_9	0.00660	0.00023	0.00074	0.00000	0.05450	0.00140	0.00676	5.3	0.00091	1.3	0.24	0.05389	5.2	6.8	0.4	5.9	0.1	366.0	116.9	14.3	**5.864**	**0.076**
MG3-25_17	0.00645	0.00020	0.00074	0.00000	0.05671	0.00120	0.00704	4.4	0.00091	1.1	0.25	0.05607	4.3	7.1	0.3	5.9	0.1	455.0	95.2	17.6	**5.871**	**0.066**
MG3-25_22	0.00635	0.00013	0.00075	0.00000	0.05627	0.00092	0.00701	3.5	0.00091	1.0	0.29	0.05564	3.3	7.1	0.2	5.9	0.1	438.0	74.5	17.0	**5.887**	**0.061**
MG3-25_2	0.00784	0.00032	0.00075	0.00000	0.07424	0.00250	0.00926	6.9	0.00092	1.3	0.19	0.07341	6.8	9.4	0.6	5.9	0.1	1025.0	137.0	37.0	**5.896**	**0.079**
MG3-25_31	0.00642	0.00016	0.00075	0.00000	0.05641	0.00079	0.00706	3.1	0.00092	1.2	0.38	0.05578	2.9	7.1	0.2	5.9	0.1	443.0	64.3	17.2	**5.918**	**0.069**
MG3-25_21	0.00530	0.00005	0.00075	0.00000	0.04792	0.00038	0.00602	2.0	0.00092	1.0	0.50	0.04738	1.7	6.1	0.1	5.9	0.1	68.0	41.3	2.6	**5.934**	**0.059**
MG3-25_25	0.00829	0.00030	0.00076	0.00000	0.05890	0.00140	0.00748	5.0	0.00093	1.2	0.25	0.05824	4.8	7.6	0.4	6.0	0.1	538.5	105.2	20.7	**6.001**	**0.075**
MG3-25_26	0.00932	0.00082	0.00076	0.00000	0.05261	0.00170	0.00671	6.6	0.00094	1.3	0.19	0.05203	6.5	6.8	0.4	6.0	0.1	286.5	148.6	11.2	**6.026**	**0.077**
MG3-25_39	0.00628	0.00016	0.00077	0.00000	0.05757	0.00120	0.00736	4.4	0.00094	1.1	0.26	0.05693	4.2	7.4	0.3	6.0	0.1	488.5	93.3	18.9	**6.044**	**0.068**
MG3-25_24	0.01205	0.00079	0.00078	0.00000	0.08398	0.00430	0.01091	10.3	0.00095	1.3	0.13	0.08304	10.3	11.0	1.1	6.1	0.1	1270.0	200.3	44.3	**6.142**	**0.080**
MG3-25_33	0.01286	0.00049	0.00079	0.00001	0.11094	0.00330	0.01458	6.2	0.00096	1.5	0.25	0.10970	6.0	14.7	0.9	6.2	0.1	1794.0	109.1	57.7	**6.209**	**0.096**
MG3-25_5	0.00606	0.00011	0.00079	0.00000	0.05101	0.00070	0.00673	3.0	0.00097	1.1	0.37	0.05044	2.8	6.8	0.2	6.2	0.1	215.0	65.6	8.4	**6.237**	**0.070**
MG3-25_13	0.00992	0.00046	0.00079	0.00000	0.07505	0.00290	0.00991	7.9	0.00097	1.4	0.18	0.07421	7.8	10.0	0.8	6.2	0.1	1047.0	156.5	37.7	**6.237**	**0.088**
MG3-25_12	0.01159	0.00030	0.00079	0.00000	0.09921	0.00180	0.01313	3.9	0.00097	1.3	0.33	0.09810	3.7	13.2	0.5	6.3	0.1	1588.0	69.1	52.8	**6.255**	**0.080**
MG3-25_14	0.01696	0.00150	0.00083	0.00001	0.12494	0.00700	0.01741	11.6	0.00102	3.0	0.26	0.12354	11.2	17.5	2.0	6.6	0.2	2008.0	199.2	62.4	**6.587**	**0.197**
MG3-25_34	0.01644	0.00076	0.00094	0.00001	0.11207	0.00300	0.01750	5.6	0.00115	1.4	0.26	0.11082	5.4	17.6	1.0	7.4	0.1	1812.5	98.1	58.1	**7.379**	**0.106**
MG3-25_32	0.04935	0.00320	0.00112	0.00003	0.27828	0.01100	0.05226	9.5	0.00138	5.2	0.55	0.27517	7.9	51.7	4.8	8.9	0.5	3335.5	124.2	82.8	**8.874**	**0.463**
MG3-25_1	0.01411	0.00023	0.00117	0.00000	0.08577	0.00140	0.01678	3.5	0.00144	1.0	0.29	0.08482	3.3	16.9	0.6	9.2	0.1	1311.0	64.8	45.3	**9.244**	**0.092**

- **Sample: MG4-1Mz (Locality: Sacaco Classic [Chacra Area]**

Crystal ID	Isotopic ratios													Estimated Ages								
	$^{207}Pb/^{235}U$*	± 1σ	$^{206}Pb/^{238}U$	± 1σ	$^{207}Pb/^{206}Pb$	± 1σ	$^{207}Pb/^{235}U$	± 2σ	$^{206}Pb/^{238}U$	± 2σ	Rho	$^{207}Pb/^{206}Pb$	± 2σ	$^{207}Pb/^{235}U$ (Ma)	± 2σ	$^{206}Pb/^{238}U$ (Ma)	± 2σ	$^{207}Pb/^{206}Pb$ (Ma)	± 2σ	% Discordance	Best age (Ma)	± 2σ
MG4-1MZ_35	0.012656	0.000900	0.000717	0.000007	0.101123	0.004500	0.012736	9.4	0.000885	2.9	0.31	0.104407	8.9	12.8	1.2	5.7	0.2	1703.5	164.6	55.6	**5.7**	**0.2**
MG4-1MZ_08	0.005897	0.000480	0.000727	0.000005	0.060974	0.001900	0.007781	6.8	0.000896	2.6	0.38	0.062954	6.3	7.9	0.5	5.8	0.1	706.5	133.7	26.6	**5.8**	**0.1**
MG4-1MZ_14	0.015718	0.001200	0.000823	0.000007	0.117406	0.004800	0.016969	8.7	0.001015	2.7	0.32	0.121218	8.2	17.1	1.5	6.5	0.2	1974.0	146.4	61.7	**6.5**	**0.2**
MG4-1MZ_15	0.004933	0.000770	0.000897	0.000007	0.061531	0.002000	0.009699	7.1	0.001107	2.6	0.37	0.063529	6.6	9.8	0.7	7.1	0.2	725.5	138.9	27.2	**7.1**	**0.2**
MG4-1MZ_26	0.006143	0.000087	0.000899	0.000004	0.046259	0.000420	0.007306	3.1	0.001109	2.4	0.76	0.047761	2.0	7.4	0.2	7.1	0.2	87.0	47.1	3.3	**7.1**	**0.2**
MG4-1MZ_19	0.012062	0.000410	0.000944	0.000006	0.081454	0.001600	0.013510	4.7	0.001165	2.5	0.53	0.084099	4.0	13.6	0.6	7.5	0.2	1294.5	78.0	44.9	**7.5**	**0.2**
MG4-1MZ_21	0.033439	0.002300	0.000985	0.000022	0.222945	0.009300	0.038576	9.7	0.001215	5.0	0.51	0.230185	8.4	38.4	3.7	7.8	0.4	3053.0	134.1	79.6	**7.8**	**0.4**
MG4-1MZ_18	0.011882	0.000270	0.001016	0.000006	0.076386	0.001200	0.013631	4.1	0.001254	2.4	0.60	0.078866	3.2	13.7	0.6	8.1	0.2	1168.5	64.2	41.3	**8.1**	**0.2**
MG4-1MZ_36	0.044409	0.003400	0.001036	0.000018	0.286125	0.008700	0.052075	7.4	0.001278	4.1	0.56	0.295416	6.1	51.5	3.7	8.2	0.3	3446.0	95.2	84.0	**8.2**	**0.3**
MG4-1MZ_17	0.011880	0.000780	0.001049	0.000008	0.079350	0.002500	0.014627	6.9	0.001295	2.6	0.38	0.081927	6.4	14.7	1.0	8.3	0.2	1243.5	124.4	43.4	**8.3**	**0.2**
MG4-1MZ_01	0.010602	0.000760	0.001145	0.000007	0.066486	0.001700	0.013373	5.7	0.001413	2.5	0.43	0.068645	5.2	13.5	0.8	9.1	0.2	888.0	107.0	32.5	**9.1**	**0.2**
MG4-1MZ_06	0.057727	0.004600	0.001147	0.000032	0.310694	0.009500	0.062590	8.6	0.001415	6.0	0.70	0.320783	6.2	61.6	5.1	9.1	0.5	3573.5	94.8	85.2	**9.1**	**0.5**
MG4-1MZ_11	0.009002	0.000480	0.001149	0.000006	0.051416	0.000990	0.010372	4.6	0.001417	2.4	0.52	0.053085	3.9	10.5	0.5	9.1	0.2	332.0	89.2	12.9	**9.1**	**0.2**
MG4-1MZ_31	0.003733	0.000920	0.001159	0.000008	0.063736	0.002000	0.012979	6.8	0.001430	2.6	0.38	0.065806	6.3	13.1	0.9	9.2	0.2	800.0	132.6	29.6	**9.2**	**0.2**
MG4-1MZ_24	0.056427	0.006400	0.001162	0.000031	0.315639	0.009500	0.064433	8.4	0.001434	5.8	0.69	0.325888	6.1	63.4	5.1	9.2	0.5	3597.5	93.2	85.4	**9.2**	**0.5**
MG4-1MZ_30	0.009063	0.000450	0.001171	0.000007	0.053460	0.001200	0.011000	5.2	0.001445	2.4	0.47	0.055196	4.6	11.1	0.6	9.3	0.2	420.0	101.8	16.2	**9.3**	**0.2**
MG4-1MZ_05	0.009686	0.000400	0.001172	0.000006	0.052090	0.001000	0.010726	4.6	0.001446	2.4	0.52	0.053781	3.9	10.8	0.5	9.3	0.2	361.5	88.5	14.0	**9.3**	**0.2**
MG4-1MZ_13	0.005374	0.000900	0.001194	0.000009	0.056338	0.002000	0.011813	7.6	0.001473	2.6	0.34	0.058168	7.1	11.9	0.9	9.5	0.2	536.0	156.4	20.4	**9.5**	**0.2**
MG4-1MZ_07	0.011910	0.000680	0.001229	0.000007	0.060764	0.001300	0.013113	5.0	0.001516	2.4	0.49	0.062738	4.4	13.2	0.7	9.8	0.2	699.0	92.7	26.2	**9.8**	**0.2**
MG4-1MZ_23	0.018671	0.000640	0.001235	0.000008	0.101817	0.002000	0.022094	4.7	0.001524	2.5	0.53	0.105123	4.0	22.2	1.0	9.8	0.2	1716.0	73.7	55.7	**9.8**	**0.2**
MG4-1MZ_16	0.010181	0.000310	0.001278	0.000008	0.053803	0.000800	0.012076	3.9	0.001577	2.5	0.63	0.055550	3.1	12.2	0.5	10.2	0.3	434.0	68.6	16.7	**10.2**	**0.3**
MG4-1MZ_29	0.024721	0.002900	0.001379	0.000009	0.145364	0.002500	0.035217	4.3	0.001702	2.5	0.58	0.150084	3.5	35.1	1.5	11.0	0.3	2346.5	60.4	68.8	**11.0**	**0.3**
MG4-1MZ_25	0.018652	0.004000	0.001511	0.000017	0.146274	0.004500	0.038812	6.9	0.001864	3.1	0.45	0.151023	6.2	38.7	2.6	12.0	0.4	2357.5	106.0	69.0	**12.0**	**0.4**
MG4-1MZ_28	0.011402	0.000330	0.001605	0.000008	0.048540	0.000760	0.013687	4.0	0.001981	2.4	0.59	0.050116	3.2	13.8	0.6	12.8	0.3	200.0	75.1	7.6	**12.8**	**0.3**
MG4-1MZ_40	0.011720	0.000410	0.001628	0.000008	0.049350	0.000620	0.014110	3.6	0.002008	2.4	0.67	0.050952	2.6	14.2	0.5	12.9	0.3	238.5	60.8	9.1	**12.9**	**0.3**
MG4-1MZ_33	0.012367	0.000310	0.001674	0.000010	0.049637	0.000610	0.014592	3.6	0.002065	2.5	0.69	0.051249	2.6	14.7	0.5	13.3	0.3	252.0	59.5	9.6	**13.3**	**0.3**
MG4-1MZ_32	0.033602	0.005600	0.001746	0.000023	0.290050	0.006400	0.088966	5.6	0.002155	3.4	0.61	0.299469	4.5	86.5	4.7	13.9	0.5	3467.0	69.5	84.0	**13.9**	**0.5**
MG4-1MZ_37	0.068967	0.005400	0.001764	0.000016	0.286526	0.003600	0.088794	3.9	0.002177	2.8	0.73	0.295830	2.6	86.4	3.2	14.0	0.4	3448.5	40.9	83.8	**14.0**	**0.4**
MG4-1MZ_02	0.118750	0.013000	0.001779	0.000036	0.496866	0.007400	0.155251	5.5	0.002195	4.6	0.83	0.513000	3.1	146.5	7.5	14.1	0.6	4279.0	45.4	90.4	**14.1**	**0.6**
MG4-1MZ_22	0.042771	0.011000	0.001808	0.000031	0.495385	0.004700	0.157355	4.5	0.002231	4.1	0.89	0.511471	2.1	148.4	6.3	14.4	0.6	4274.5	30.3	90.3	**14.4**	**0.6**
MG4-1MZ_27	0.032785	0.004300	0.001925	0.000030	0.137107	0.007500	0.046357	11.6	0.002375	3.8	0.33	0.141559	11.0	46.0	5.2	15.3	0.6	2246.0	189.6	66.8	**15.3**	**0.6**
MG4-1MZ_04	0.060465	0.008800	0.003396	0.000023	0.122276	0.003600	0.072933	6.5	0.004190	2.6	0.40	0.126246	5.9	71.5	4.5	27.0	0.7	2046.0	105.0	62.3	**27.0**	**0.7**
MG4-1MZ_10	0.100372	0.017000	0.004630	0.000330	0.487127	0.012000	0.396119	15.3	0.005712	14.4	0.95	0.502945	5.0	338.8	43.5	36.7	5.3	4249.5	73.5	89.2	**36.7**	**5.3**
MG4-1MZ_09	0.220654	0.049000	0.005809	0.000110	0.649048	0.004000	0.662221	4.6	0.007167	4.4	0.95	0.670123	1.5	515.9	18.5	46.0	2.0	4600.0	22.3	91.1	**46.0**	**2.0**
MG4-1MZ_34	0.023669	0.013000	0.006031	0.000410	0.458522	0.012000	0.485695	14.8	0.007441	13.8	0.93	0.473412	5.3	402.0	48.4	47.8	6.6	4160.0	78.4	88.1	**47.8**	**6.6**
MG4-1MZ_03	0.093975	0.004200	0.011764	0.000057	0.047862	0.000320	0.098893	2.8	0.014514	2.4	0.84	0.049416	1.6	95.7	2.6	92.9	2.2	167.5	36.4	3.0	**92.9**	**2.2**
MG4-1MZ_38	0.128507	0.003700	0.017009	0.000086	0.047592	0.000170	0.142180	2.6	0.020986	2.4	0.91	0.049138	1.1	135.0	3.3	133.9	3.2	154.0	25.2	0.8	**133.9**	**3.2**
MG4-1MZ_20	0.125277	0.003400	0.017110	0.000071	0.048378	0.000240	0.145388	2.6	0.021111	2.3	0.88	0.049948	1.3	137.8	3.4	134.7	3.1	192.5	29.7	2.3	**134.7**	**3.1**
MG4-1MZ_12	0.106989	0.008500	0.017917	0.000091	0.047249	0.000210	0.148693	2.7	0.022106	2.4	0.89	0.048784	1.2	140.8	3.5	140.9	3.3	137.0	28.2	-0.1	**140.9**	**3.3**
MG4-1MZ_39	0.612808	0.019000	0.075054	0.000390	0.058226	0.000110	0.767556	2.6	0.092601	2.4	0.94	0.060116	0.9	578.3	11.3	570.9	13.1	607.5	19.2	1.3	**570.9**	**13.1**

- **Sample: MG3-57 (Locality: Cerro Amarillo)**

Crystal ID	Isotopic ratios													Estimated Ages								
	$^{207}Pb/^{235}U$*	± 1σ	$^{206}Pb/^{238}U$	± 1σ	$^{207}Pb/^{206}Pb$	± 1σ	$^{207}Pb/^{235}U$	± 2σ	$^{206}Pb/^{238}U$	± 2σ	Rho	$^{207}Pb/^{206}Pb$	± 2σ	$^{207}Pb/^{235}U$ (Ma)	± 2σ	$^{206}Pb/^{238}U$ (Ma)	± 2σ	$^{207}Pb/^{206}Pb$ (Ma)	± 2σ	% Discordance	Best age (Ma)	± 2σ
MG3-57_13	-0.00144	0.00090	0.16190	0.00027	0.11508	0.02600	0.00493	46.7	0.00030	11.5	0.25	0.11741	45.2	5.0	2.3	1.96	0.2	1917.0	810.6	60.7	**1.964**	**0.225**
MG3-57_40	0.01133	0.00037	0.00035	0.00000	0.27225	0.00510	0.01549	4.7	0.00040	2.7	0.58	0.27777	3.8	15.6	0.7	2.6	0.1	3350.0	59.8	83.3	**2.606**	**0.071**
MG3-57_10	0.02038	0.00260	0.00047	0.00001	0.39991	0.00820	0.03021	5.7	0.00054	3.9	0.68	0.40802	4.2	30.2	1.7	3.5	0.1	3938.5	62.7	88.5	**3.460**	**0.134**
MG3-57_32	0.00802	0.00079	0.00085	0.00001	0.05595	0.00250	0.00770	9.3	0.00098	2.5	0.27	0.05708	9.0	7.8	0.7	6.3	0.2	494.5	197.7	19.1	**6.306**	**0.157**
MG3-57_35	0.03887	0.00440	0.00094	0.00005	0.26907	0.01500	0.04069	15.7	0.00107	11.1	0.70	0.27453	11.2	40.5	6.2	6.9	0.8	3332.0	174.9	82.9	**6.926**	**0.766**
MG3-57_36	0.00958	0.00030	0.00111	0.00000	0.05524	0.00100	0.00988	4.3	0.00127	2.2	0.51	0.05636	3.7	10.0	0.4	8.2	0.2	466.5	82.0	18.0	**8.189**	**0.179**
MG3-57_17	0.00524	0.00140	0.00027	0.00121	0.05515	0.00170	0.01078	6.7	0.00139	2.5	0.37	0.05627	6.2	10.9	0.7	9.0	0.2	462.5	137.7	17.8	**8.954**	**0.223**
MG3-57_03	0.01114	0.00030	0.00124	0.00001	0.04962	0.00093	0.00990	4.4	0.00142	2.2	0.50	0.05063	3.8	10.0	0.4	9.1	0.2	224.0	88.5	8.7	**9.132**	**0.203**
MG3-57_20	0.01139	0.00092	0.01167	0.00125	0.05538	0.00150	0.01114	5.9	0.00143	2.2	0.37	0.05650	5.5	11.2	0.7	9.2	0.2	472.0	121.1	18.1	**9.209**	**0.202**
MG3-57_38	0.01196	0.00120	0.00125	0.00001	0.04916	0.00120	0.00994	5.4	0.00144	2.3	0.42	0.05015	4.9	10.0	0.5	9.3	0.2	202.0	114.8	7.8	**9.259**	**0.210**
MG3-57_02	0.00657	0.00092	0.00132	0.00001	0.07564	0.00340	0.01611	9.4	0.00151	2.5	0.27	0.07718	9.0	16.2	1.5	9.8	0.2	1125.5	179.8	39.9	**9.753**	**0.248**
MG3-57_29	0.01047	0.00022	0.00138	0.00000	0.04916	0.00013	0.01043	3.2	0.00159	2.1	0.67	0.04771	2.4	10.5	0.3	10.2	0.2	84.5	55.9	3.1	**10.217**	**0.219**
MG3-57_14	-0.00119	0.00100	0.16193	0.00156	0.07377	0.00430	0.01853	12.0	0.00179	2.6	0.21	0.07527	11.7	18.6	2.2	11.5	0.3	1075.5	234.6	38.3	**11.500**	**0.294**
MG3-57_15	0.01545	0.00062	0.01196	0.00176	0.05009	0.00098	0.01426	4.6	0.00202	2.3	0.49	0.05110	4.0	14.4	0.7	13.0	0.3	245.0	91.9	9.3	**13.030**	**0.294**
MG3-57_25	0.01240	0.00046	0.00177	0.00001	0.67020	0.01000	0.01353	4.8	0.00203	2.2	0.45	0.04831	4.3	13.6	0.7	13.1	0.3	114.5	101.3	4.1	**13.082**	**0.283**
MG3-57_33	0.04956	0.00420	0.00180	0.00005	0.21429	0.01200	0.06214	12.6	0.00206	5.7	0.45	0.21864	11.2	61.2	7.5	13.3	0.8	2970.5	180.9	78.3	**13.273**	**0.758**
MG3-57_22	0.01438	0.00059	0.00182	0.00001	0.04822	0.00039	0.01778	3.6	0.00209	2.2	0.61	0.06161	2.9	17.9	0.6	13.5	0.3	660.5	61.9	24.7	**13.476**	**0.299**
MG3-57_24	0.01480	0.01200	0.00195	0.00015	0.04728	0.00071	0.21108	15.8	0.00224	15.5	0.98	0.68380	3.1	194.4	27.8	14.4	2.2	4600.0	47.7	92.6	**14.416**	**2.232**
MG3-57_31	0.01563	0.00023	0.00226	0.00001	0.04586	0.00034	0.01673	2.8	0.00259	2.2	0.79	0.04679	1.7	16.8	0.5	16.7	0.4	38.5	40.1	0.9	**16.692**	**0.365**
MG3-57_04	0.02393	0.00950	0.00265	0.00023	0.31222	0.01900	0.13364	21.3	0.00304	17.5	0.82	0.31855	12.2	127.4	25.3	19.6	3.4	3562.5	187.7	84.6	**19.584**	**3.413**
MG3-57_23	0.01983	0.00140	0.00299	0.00001	0.06039	0.00084	0.02280	3.8	0.00343	2.2	0.57	0.04824	3.1	22.9	0.9	22.1	0.5	111.0	73.3	3.6	**22.061**	**0.478**
MG3-57_12	0.02572	0.00078	0.00047	0.00300	0.05144	0.00084	0.02488	4.0	0.00344	2.2	0.55	0.05249	3.4	25.0	1.0	22.1	0.5	306.5	76.5	11.3	**22.127**	**0.485**
MG3-57_09	0.03101	0.00110	0.00302	0.00001	0.04935	0.00073	0.02403	3.8	0.00346	2.2	0.59	0.05035	3.1	24.1	0.9	22.3	0.5	211.0	70.9	7.6	**22.277**	**0.493**
MG3-57_19	0.01683	0.00120	0.00176	0.00327	0.04566	0.00090	0.02408	4.6	0.00375	2.2	0.48	0.04658	4.0	24.2	1.1	24.1	0.5	27.5	96.4	0.2	**24.125**	**0.528**
MG3-57_39	0.03981	0.00220	0.00567	0.00002	0.04847	0.00055	0.04432	3.2	0.00650	2.1	0.67	0.04945	2.4	44.0	1.4	41.8	0.9	169.0	56.1	5.2	**41.767**	**0.895**
MG3-57_26	0.05840	0.00190	0.00891	0.00004	0.04735	0.00100	0.06791	2.6	0.01022	2.2	0.85	0.04820	1.4	66.7	1.7	65.5	1.4	108.5	32.7	1.8	**65.538**	**1.432**
MG3-57_30	0.07892	0.00290	0.00992	0.00005	0.04676	0.00052	0.07340	2.7	0.01137	2.2	0.84	0.04681	1.4	71.9	1.8	72.9	1.6	39.5	34.7	-1.4	**72.889**	**1.620**
MG3-57_16	0.04796	0.00710	0.00300	0.01167	0.04924	0.00035	0.09271	2.7	0.01338	2.1	0.80	0.05024	1.6	90.0	2.3	85.7	1.8	206.0	37.6	4.8	**85.699**	**1.821**
MG3-57_07	0.11248	0.01300	0.01176	0.00004	0.04965	0.00042	0.09422	2.8	0.01349	2.1	0.75	0.05066	1.9	91.4	2.5	86.4	1.8	225.0	43.1	5.5	**86.369**	**1.834**
MG3-57_34	0.06434	0.00550	0.01181	0.00004	0.04915	0.00047	0.09366	3.0	0.01355	2.1	0.72	0.05014	2.1	90.9	2.6	86.7	1.8	201.5	48.0	4.6	**86.742**	**1.837**
MG3-57_27	0.08596	0.00260	0.01182	0.00005	0.04724	0.00027	0.09077	2.5	0.01356	2.2	0.88	0.04856	1.2	88.2	2.1	86.8	1.9	126.0	27.7	1.6	**86.812**	**1.880**
MG3-57_21	0.05645	0.00540	0.01193	0.00004	0.05515	0.00170	0.09278	2.8	0.01368	2.1	0.77	0.04920	1.8	90.1	2.4	87.6	1.9	157.0	42.0	2.8	**87.567**	**1.857**
MG3-57_11	0.08703	0.00480	0.00302	0.01196	0.04761	0.00034	0.09185	2.7	0.01371	2.1	0.79	0.04858	1.6	89.2	2.3	87.8	1.9	127.5	38.3	1.6	**87.790**	**1.857**
MG3-57_01	0.07551	0.00990	0.01198	0.00004	0.04669	0.00031	0.09024	2.6	0.01374	2.1	0.81	0.04763	1.5	87.7	2.2	88.0	1.9	81.0	36.6	-0.3	**87.965**	**1.864**
MG3-57_06	0.15424	0.00460	0.01796	0.00006	0.04785	0.00022	0.13867	2.5	0.02060	2.1	0.87	0.04882	1.2	131.8	3.0	131.4	2.8	139.0	28.3	0.3	**131.440**	**2.783**
MG3-57_05	0.16230	0.00550	0.01825	0.00005	0.04747	0.00021	0.13981	2.4	0.02093	2.1	0.87	0.04844	1.2	132.9	3.0	133.6	2.8	120.5	27.8	-0.5	**133.556**	**2.807**
MG3-57_08	0.16913	0.00470	0.01866	0.00006	0.04883	0.00024	0.14705	2.5	0.02141	2.1	0.86	0.04982	1.3	139.3	3.2	136.5	2.9	186.5	29.2	2.0	**136.526**	**2.880**
MG3-57_37	0.20494	0.01400	0.01942	0.00009	0.07835	0.00130	0.24546	4.1	0.02227	2.2	0.55	0.07994	3.4	222.9	8.1	142.0	3.1	1195.0	67.3	36.3	**141.983**	**3.132**
MG3-57_28	0.13625	0.00240	0.01945	0.00009	0.04759	0.00021	0.15423	2.4	0.02230	2.2	0.92	0.05016	0.9	145.6	3.3	142.2	3.1	202.0	21.9	2.4	**142.184**	**3.142**
MG3-57_18	0.39330	0.02900	0.00156	0.06740	0.05591	0.00013	0.60787	2.3	0.07729	2.2	0.92	0.05704	0.9	482.2	9.0	479.9	10.0	493.0	20.0	0.5	**479.924**	**10.001**

- **Sample: MG3-09 (Locality: Cerro Amarillo)**

Crystal ID	Isotopic ratios													Estimated Ages									
	$^{207}Pb/^{235}U$ *	± 1σ	$^{206}Pb/^{238}U$	± 1σ	$^{207}Pb/^{206}Pb$	± 1σ	$^{207}Pb/^{235}U$	± 2σ	$^{206}Pb/^{238}U$	± 2σ	Rho	$^{207}Pb/^{206}Pb$	± 2σ	$^{207}Pb/^{235}U$ (Ma)	± 2σ	$^{206}Pb/^{238}U$ (Ma)	± 2σ	$^{207}Pb/^{206}Pb$ (Ma)	± 2σ	% Discordanc	Best age (Ma)	± 2σ
MG3-09_26	0.006721	0.000270	0.000664	0.000004	0.059767	0.001500	0.007039	5.5	0.000825	2.1	0.38	0.061895	5.0	7.1	0.4	5.3	0.1	670.0	108.0	25.4	**5.3**	**0.1**
MG3-09_05	0.005439	0.000140	0.000704	0.000003	0.052577	0.001000	0.006567	4.3	0.000875	1.9	0.45	0.054450	3.8	6.6	0.3	5.6	0.1	389.5	86.1	15.2	**5.6**	**0.1**
MG3-09_14	0.006245	0.000260	0.000739	0.000004	0.049283	0.000990	0.006464	4.5	0.000919	2.0	0.44	0.051038	4.0	6.5	0.3	5.9	0.1	242.5	93.3	9.5	**5.9**	**0.1**
MG3-09_08	0.012804	0.002700	0.000831	0.000035	0.477444	0.013000	0.070377	10.2	0.001032	8.6	0.84	0.494450	5.5	69.1	6.8	6.7	0.6	4224.5	80.7	90.4	**6.7**	**0.6**
MG3-09_12	0.011094	0.004000	0.000897	0.000037	0.387092	0.016000	0.061624	11.8	0.001115	8.4	0.71	0.400880	8.3	60.7	7.0	7.2	0.6	3912.0	124.5	88.2	**7.2**	**0.6**
MG3-09_13	0.012714	0.000530	0.001074	0.000006	0.083527	0.001700	0.015917	4.6	0.001335	2.1	0.45	0.086502	4.1	16.0	0.7	8.6	0.2	1349.0	79.2	46.4	**8.6**	**0.2**
MG3-09_19	0.008092	0.000300	0.001143	0.000006	0.047445	0.000810	0.009619	4.0	0.001420	2.0	0.50	0.049135	3.5	9.7	0.4	9.1	0.2	154.0	80.8	5.9	**9.1**	**0.2**
MG3-09_10	0.010479	0.000510	0.001166	0.000006	0.051799	0.001100	0.010715	4.7	0.001449	1.9	0.41	0.053644	4.3	10.8	0.5	9.3	0.2	356.0	96.6	13.8	**9.3**	**0.2**
MG3-09_25	0.008349	0.001000	0.001190	0.000007	0.075161	0.001400	0.015866	4.3	0.001478	2.1	0.48	0.077838	3.8	16.0	0.7	9.5	0.2	1142.5	74.7	40.4	**9.5**	**0.2**
MG3-09_04	0.012931	0.000850	0.001200	0.000007	0.071482	0.001900	0.015221	5.7	0.001491	2.1	0.36	0.074028	5.3	15.3	0.9	9.6	0.2	1042.0	107.7	37.4	**9.6**	**0.2**
MG3-09_33	0.010791	0.000280	0.001524	0.000007	0.053458	0.000650	0.014447	3.1	0.001893	1.9	0.61	0.055362	2.5	14.6	0.5	12.2	0.2	426.5	55.4	16.3	**12.2**	**0.2**
MG3-09_15	0.012279	0.000820	0.001546	0.000008	0.049388	0.000970	0.013544	4.4	0.001921	2.0	0.45	0.051147	4.0	13.7	0.6	12.4	0.2	247.0	91.2	9.5	**12.4**	**0.2**
MG3-09_34	0.011164	0.000140	0.001594	0.000006	0.047900	0.000390	0.013541	2.5	0.001980	1.9	0.74	0.049606	1.7	13.7	0.3	12.7	0.2	176.5	39.7	6.6	**12.7**	**0.2**
MG3-09_03	0.011443	0.000270	0.001621	0.000007	0.047038	0.000470	0.013523	2.8	0.002013	1.9	0.67	0.048713	2.1	13.6	0.4	13.0	0.2	134.0	48.4	4.9	**13.0**	**0.2**
MG3-09_18	0.013177	0.000770	0.001638	0.000008	0.048235	0.000740	0.014015	3.7	0.002035	1.9	0.53	0.049953	3.1	14.1	0.5	13.1	0.3	192.5	72.3	7.3	**13.1**	**0.3**
MG3-09_09	0.015551	0.000450	0.001672	0.000007	0.060198	0.000760	0.017853	3.2	0.002077	1.9	0.59	0.062342	2.6	18.0	0.6	13.4	0.3	685.5	54.9	25.6	**13.4**	**0.3**
MG3-09_11	0.021050	0.002500	0.001700	0.000014	0.102001	0.003000	0.030756	6.4	0.002112	2.4	0.37	0.105634	5.9	30.8	1.9	13.6	0.3	1725.0	108.4	55.8	**13.6**	**0.3**
MG3-09_07	0.012982	0.000310	0.001703	0.000008	0.054484	0.000720	0.016461	3.3	0.002116	1.9	0.58	0.056425	2.7	16.6	0.5	13.6	0.3	469.0	59.5	17.8	**13.6**	**0.3**
MG3-09_06	0.026104	0.003800	0.002340	0.000015	0.150145	0.002400	0.062312	3.9	0.002906	2.1	0.55	0.155493	3.2	61.4	2.3	18.7	0.4	2407.0	55.0	69.5	**18.7**	**0.4**
MG3-09_21	0.000983	0.003100	0.002484	0.000140	0.413025	0.018000	0.182009	14.4	0.003086	11.4	0.79	0.427737	8.7	169.8	22.3	19.9	2.3	4009.5	130.4	88.3	**19.9**	**2.3**
MG3-09_22	0.144389	0.027000	0.004993	0.000230	0.367668	0.014000	0.325658	12.1	0.006203	9.4	0.78	0.380764	7.6	286.2	29.9	39.9	3.7	3834.5	115.3	86.1	**39.9**	**3.7**
MG3-09_16	0.066393	0.002800	0.008212	0.000037	0.053339	0.000520	0.077701	2.8	0.010202	1.9	0.69	0.055239	2.0	76.0	2.0	65.4	1.2	421.5	44.9	13.9	**65.4**	**1.2**
MG3-09_17	0.006985	0.004100	0.008439	0.000042	0.049476	0.000700	0.074066	3.5	0.010484	2.0	0.56	0.051239	2.9	72.5	2.4	67.2	1.3	251.5	66.1	7.3	**67.2**	**1.3**
MG3-09_20	0.071553	0.003200	0.008508	0.000036	0.046133	0.000250	0.069624	2.2	0.010569	1.9	0.85	0.047776	1.2	68.3	1.5	67.8	1.3	88.0	28.3	0.8	**67.8**	**1.3**
MG3-09_29	0.057571	0.001700	0.008613	0.000036	0.046128	0.000260	0.070476	2.3	0.010700	1.9	0.84	0.047771	1.2	69.1	1.5	68.6	1.3	87.5	29.2	0.8	**68.6**	**1.3**
MG3-09_28	0.052950	0.005100	0.008976	0.000038	0.046283	0.000310	0.073692	2.4	0.011150	1.9	0.80	0.047932	1.4	72.2	1.7	71.5	1.3	95.5	33.8	1.0	**71.5**	**1.3**
MG3-09_31	0.050393	0.006000	0.009383	0.000042	0.047882	0.000300	0.079697	2.3	0.011657	1.9	0.82	0.049587	1.3	77.9	1.8	74.7	1.4	175.5	31.4	4.0	**74.7**	**1.4**
MG3-09_24	0.021135	0.004900	0.009669	0.000041	0.046485	0.000450	0.079725	2.8	0.012011	1.9	0.69	0.048140	2.0	77.9	2.1	77.0	1.4	106.0	47.2	1.2	**77.0**	**1.4**
MG3-09_30	0.008470	0.002600	0.010216	0.000052	0.049504	0.000740	0.089710	3.6	0.012691	2.0	0.55	0.051267	3.0	87.2	3.0	81.3	1.6	252.5	69.7	6.8	**81.3**	**1.6**
MG3-09_37	0.017287	0.004000	0.010349	0.000047	0.051013	0.000700	0.093645	3.4	0.012856	1.9	0.57	0.052830	2.8	90.9	2.9	82.3	1.6	321.0	63.4	9.4	**82.3**	**1.6**
MG3-09_23	0.055971	0.005800	0.010357	0.000042	0.046652	0.000280	0.085710	2.3	0.012867	1.9	0.82	0.048313	1.3	83.5	1.8	82.4	1.5	114.5	30.6	1.3	**82.4**	**1.5**
MG3-09_32	0.051559	0.006300	0.011082	0.000049	0.047094	0.000270	0.092579	2.3	0.013767	1.9	0.84	0.048772	1.2	89.9	2.0	88.1	1.7	136.5	29.4	2.0	**88.1**	**1.7**
MG3-09_02	0.019671	0.006000	0.016267	0.000073	0.048894	0.000490	0.141085	2.8	0.020208	1.9	0.68	0.050635	2.1	134.0	3.5	129.0	2.4	224.0	47.7	3.8	**129.0**	**2.4**
MB3-09_40	0.118806	0.003700	0.016815	0.000059	0.047348	0.000180	0.141226	2.0	0.020889	1.8	0.90	0.049035	0.9	134.1	2.6	133.3	2.4	149.0	21.3	0.6	**133.3**	**2.4**
MB3-09_39	0.117636	0.001900	0.016878	0.000059	0.046885	0.000110	0.140369	2.0	0.020967	1.8	0.94	0.048555	0.7	133.4	2.4	133.8	2.4	126.0	16.1	-0.3	**133.8**	**2.4**
MG3-09_36	0.022052	0.009400	0.017133	0.000078	0.049084	0.000360	0.149173	2.5	0.021284	1.9	0.78	0.050832	1.5	141.2	3.2	135.8	2.6	233.0	35.7	3.8	**135.8**	**2.6**
MG3-09_38	0.125726	0.004100	0.017323	0.000073	0.047228	0.000160	0.145125	2.1	0.021520	1.9	0.91	0.048911	0.8	137.6	2.7	137.2	2.6	143.5	19.7	0.2	**137.2**	**2.6**
MG3-09_35	0.122219	0.003100	0.017863	0.000066	0.047880	0.000170	0.151717	2.0	0.022191	1.8	0.91	0.049586	0.9	143.4	2.7	141.5	2.6	175.5	20.2	1.3	**141.5**	**2.6**
MG3-09_01	1.045046	0.024000	0.103328	0.000350	0.064086	0.000083	1.174646	1.9	0.128363	1.8	0.96	0.066369	0.6	788.8	10.4	778.5	13.3	818.0	11.7	1.3	**778.5**	**13.3**
MG3-09_27	11.636180	1.700000	0.468388	0.002100	0.231695	0.000097	19.250690	2.0	0.581873	1.9	0.97	0.239948	0.5	3054.3	19.0	2956.3	45.3	3119.5	8.0	3.2	**2956.3**	**45.3**

- **Sample: MG-117A (Locality: Quebrada Caracoles**

Crystal ID	Isotopic ratios													Estimated Ages								
	$^{207}Pb/^{235}U$*	± 1σ	$^{206}Pb/^{238}U$	± 1σ	$^{207}Pb/^{206}Pb$	± 1σ	$^{207}Pb/^{235}U$	± 2σ	$^{206}Pb/^{238}U$	± 2σ	Rho	$^{207}Pb/^{206}Pb$	± 2σ	$^{207}Pb/^{235}U$ (Ma)	± 2σ	$^{206}Pb/^{238}U$ (Ma)	± 2σ	$^{207}Pb/^{206}Pb$ (Ma)	± 2σ	% Discordance	Best age (Ma)	± 2σ
MG-117A_14	0.00509	0.00008	0.00060	0.00000	0.05017	0.00076	0.00484	3.5	0.00069	1.6	0.46	0.05058	3.1	4.9	0.2	4.5	0.1	221.5	71.4	8.8	**4.472**	**0.071**
MG-117A_27	0.00638	0.00040	0.00062	0.00000	0.04951	0.00180	0.00497	7.6	0.00072	2.0	0.27	0.04991	7.3	5.0	0.4	4.7	0.1	190.5	169.7	7.6	**4.653**	**0.093**
MG-117A_22	0.03993	0.00220	0.00079	0.00002	0.20427	0.00800	0.02596	9.0	0.00091	4.3	0.48	0.20594	7.9	26.0	2.3	5.9	0.3	2873.5	127.7	77.4	**5.890**	**0.254**
MG-117A_38	0.00995	0.00019	0.00121	0.00001	0.08120	0.00280	0.01589	7.2	0.00141	1.8	0.26	0.08186	6.9	16.0	1.1	9.1	0.2	1242.0	135.6	43.3	**9.068**	**0.167**
MG-117A_07	0.01033	0.00030	0.00126	0.00001	0.05778	0.00130	0.01178	4.8	0.00147	1.7	0.34	0.05825	4.5	11.9	0.6	9.4	0.2	539.0	99.3	20.5	**9.449**	**0.156**
MG-117A_35	0.00918	0.00026	0.00130	0.00000	0.05133	0.00091	0.01080	3.9	0.00151	1.6	0.40	0.05175	3.6	10.9	0.4	9.7	0.2	274.5	82.4	10.6	**9.745**	**0.154**
MG-117A_17	0.02442	0.00100	0.00139	0.00001	0.09813	0.00300	0.02211	6.4	0.00162	2.0	0.30	0.09893	6.1	22.2	1.4	10.4	0.2	1604.0	114.6	53.0	**10.440**	**0.204**
MG-117A_30	0.01168	0.00078	0.00154	0.00001	0.06880	0.00310	0.01717	9.3	0.00179	2.1	0.23	0.06937	9.0	17.3	1.6	11.6	0.2	909.5	186.0	33.1	**11.560**	**0.243**
MG-117A_15	0.16818	0.03700	0.00433	0.00006	0.41193	0.00580	0.28894	4.2	0.00505	3.1	0.73	0.41529	2.9	257.7	9.6	32.4	1.0	3965.0	43.1	87.4	**32.446**	**1.007**
MG-117A_29	0.06096	0.00140	0.00914	0.00003	0.04670	0.00021	0.06905	1.9	0.01064	1.6	0.82	0.04708	1.1	67.8	1.2	68.2	1.1	53.0	25.7	-0.6	**68.208**	**1.060**
MG-117A_31	0.05996	0.00150	0.00925	0.00002	0.04704	0.00017	0.07043	1.8	0.01077	1.5	0.85	0.04742	0.9	69.1	1.2	69.1	1.0	70.5	22.3	0.1	**69.057**	**1.036**
MG-117A_12	0.06896	0.00085	0.00935	0.00003	0.04715	0.00017	0.07134	1.8	0.01088	1.6	0.86	0.04754	0.9	70.0	1.2	69.8	1.1	76.0	22.2	0.3	**69.779**	**1.092**
MG-117A_25	0.07994	0.00180	0.00943	0.00002	0.04698	0.00023	0.07169	1.9	0.01098	1.5	0.79	0.04736	1.1	70.3	1.3	70.4	1.0	67.5	27.3	-0.1	**70.379**	**1.044**
MG-117A_08	0.11149	0.00280	0.00986	0.00006	0.07904	0.00120	0.12613	3.6	0.01148	1.8	0.50	0.07968	3.1	120.6	4.1	73.6	1.3	1189.0	61.1	39.0	**73.585**	**1.319**
MG-117A_06	0.08724	0.00260	0.01024	0.00003	0.04873	0.00031	0.08077	2.1	0.01192	1.6	0.74	0.04913	1.4	78.9	1.6	76.4	1.2	153.5	32.9	3.1	**76.413**	**1.189**
MG-117A_26	0.08559	0.00310	0.01044	0.00003	0.04874	0.00029	0.08233	2.0	0.01215	1.5	0.75	0.04914	1.3	80.3	1.6	77.9	1.2	154.5	31.2	3.1	**77.854**	**1.183**
MG-117A_40	0.06497	0.00180	0.01069	0.00003	0.04738	0.00015	0.08198	1.7	0.01245	1.5	0.87	0.04777	0.9	80.0	1.3	79.7	1.2	87.5	20.6	0.3	**79.742**	**1.197**
MG-117A_36	0.08333	0.00210	0.01167	0.00003	0.04733	0.00014	0.08939	1.7	0.01359	1.5	0.87	0.04772	0.8	86.9	1.4	87.0	1.3	85.0	19.9	-0.1	**86.999**	**1.302**
MG-117A_16	0.11061	0.00270	0.01253	0.00005	0.04800	0.00023	0.09729	2.0	0.01458	1.6	0.82	0.04839	1.1	94.3	1.8	93.3	1.5	118.0	26.6	1.0	**93.320**	**1.514**
MG-117A_20	0.14128	0.00390	0.01308	0.00004	0.05009	0.00022	0.10604	1.9	0.01523	1.5	0.82	0.05050	1.1	102.3	1.8	97.4	1.5	218.0	24.6	4.8	**97.429**	**1.470**
MG-117A_05	0.14757	0.00520	0.01581	0.00007	0.04945	0.00018	0.12650	1.9	0.01840	1.7	0.87	0.04985	0.9	120.9	2.2	117.6	2.0	188.0	21.9	2.8	**117.550**	**1.978**
MG-117A_02	0.12439	0.00410	0.01806	0.00005	0.04915	0.00025	0.14360	1.9	0.02102	1.5	0.79	0.04955	1.2	136.2	2.5	134.1	2.0	173.5	27.5	1.6	**134.097**	**2.024**
MG-117A_03	0.12710	0.00180	0.01808	0.00005	0.05016	0.00012	0.14680	1.7	0.02105	1.5	0.89	0.05057	0.8	139.1	2.2	134.3	2.0	221.0	17.7	3.4	**134.303**	**2.016**
MG-117A_09	0.15076	0.00590	0.01821	0.00006	0.04821	0.00016	0.14210	1.8	0.02120	1.5	0.87	0.04860	0.9	134.9	2.3	135.3	2.1	128.5	21.0	-0.3	**135.255**	**2.073**
MG-117A_01	0.16617	0.00320	0.01837	0.00007	0.05871	0.00065	0.17453	2.8	0.02139	1.6	0.58	0.05919	2.3	163.3	4.2	136.4	2.2	573.5	49.9	16.5	**136.409**	**2.200**
MG-117A_23	0.17495	0.00540	0.01841	0.00005	0.04894	0.00019	0.14577	1.8	0.02143	1.5	0.84	0.04934	1.0	138.2	2.3	136.7	2.0	163.5	22.9	1.1	**136.677**	**2.047**
MG-117A_24	0.15246	0.00270	0.01847	0.00007	0.04857	0.00014	0.14516	1.8	0.02150	1.6	0.89	0.04897	0.8	137.6	2.3	137.1	2.1	146.0	19.4	0.4	**137.114**	**2.146**
MG-117A_39	0.11404	0.00210	0.01852	0.00006	0.04798	0.00010	0.14382	1.7	0.02156	1.5	0.90	0.04837	0.7	136.4	2.2	137.5	2.1	117.0	17.1	-0.8	**137.528**	**2.096**
MG-117A_21	0.18836	0.00260	0.01861	0.00005	0.04895	0.00015	0.14738	1.7	0.02166	1.5	0.87	0.04935	0.9	139.6	2.3	138.1	2.1	164.0	20.0	1.0	**138.143**	**2.071**
MG-117A_04	0.15052	0.00380	0.01884	0.00006	0.04867	0.00015	0.14836	1.8	0.02193	1.6	0.88	0.04906	0.9	140.5	2.3	139.8	2.1	150.5	20.1	0.4	**139.845**	**2.149**
MG-117A_18	0.17070	0.00340	0.01890	0.00005	0.04930	0.00025	0.15079	1.9	0.02200	1.5	0.79	0.04970	1.2	142.6	2.5	140.3	2.1	180.5	27.4	1.6	**140.310**	**2.094**
MG-117A_33	0.18808	0.00650	0.01897	0.00010	0.07236	0.00150	0.22217	4.5	0.02209	1.8	0.39	0.07295	4.2	203.7	8.4	140.8	2.5	1012.5	84.9	30.9	**140.832**	**2.460**
MG-117A_28	0.15277	0.00360	0.01903	0.00005	0.04958	0.00019	0.15270	1.8	0.02215	1.5	0.84	0.04999	1.0	144.3	2.4	141.2	2.1	194.5	22.6	2.1	**141.250**	**2.106**
MG-117A_13	0.43971	0.01100	0.03238	0.00053	0.08047	0.00091	0.42166	4.3	0.03770	3.6	0.84	0.08113	2.3	357.2	12.8	238.5	8.4	1224.5	45.9	33.2	**238.529**	**8.350**
MG-117A_34	0.52336	0.01400	0.06661	0.00015	0.05532	0.00009	0.59634	1.6	0.07755	1.5	0.91	0.05577	0.7	474.9	6.2	481.5	6.9	443.0	15.1	-1.4	**481.454**	**6.896**
MG-117A_19	0.83228	0.01000	0.07053	0.00042	0.06009	0.00007	0.68588	2.0	0.08211	1.9	0.94	0.06058	0.6	530.3	8.1	508.7	9.1	624.0	13.9	4.1	**508.706**	**9.051**
MG-117A_11	0.63279	0.02100	0.07223	0.00022	0.05705	0.00009	0.66687	1.7	0.08408	1.5	0.91	0.05752	0.7	518.8	6.8	520.4	7.7	511.5	15.0	-0.3	**520.433**	**7.709**
MG-117A_10	0.08332	0.06900	0.08499	0.00026	0.05980	0.00016	0.82244	1.7	0.09894	1.5	0.89	0.06029	0.8	609.4	8.0	608.2	9.0	613.5	17.3	0.2	**608.190**	**8.955**
MG-117A_32	2.11044	0.09700	0.17815	0.00054	0.07947	0.00007	2.29099	1.7	0.20740	1.5	0.93	0.08012	0.6	1209.5	11.7	1214.9	17.1	1199.5	12.3	-0.4	**1214.891**	**17.054**

- **Sample: MG-138A (Locality: Yauca)**

Crystal ID	Isotopic ratios														Estimated Ages								
	$^{207}Pb/^{235}U$*	± 1σ	$^{206}Pb/^{238}U$	± 1σ	$^{207}Pb/^{206}Pb$	± 1σ	$^{207}Pb/^{235}U$	± 2σ	$^{206}Pb/^{238}U$	± 2σ	Rho	$^{207}Pb/^{206}Pb$	± 2σ	$^{207}Pb/^{235}U$ (Ma)	± 2σ	$^{206}Pb/^{238}U$ (Ma)	± 2σ	$^{207}Pb/^{206}Pb$ (Ma)	± 2σ	% Discordance	Best age (Ma)	± 2σ
MG-138A_15	0.00108	0.00047	0.00059	0.00001	0.08777	0.00550	0.00858	12.8	0.00072	2.3	0.18	0.08679	12.6	8.7	1.1	4.6	0.1	1355.5	242.1	46.7	**4.620**	**0.108**
MG-138A_20	0.00617	0.00045	0.00059	0.00000	0.06204	0.00280	0.00611	9.2	0.00072	1.7	0.18	0.06135	9.1	6.2	0.6	4.7	0.1	651.5	194.3	24.7	**4.654**	**0.078**
MG-138A_16	0.00304	0.00100	0.00060	0.00001	0.10342	0.00560	0.01029	11.1	0.00073	2.1	0.19	0.10226	10.9	10.4	1.1	4.7	0.1	1665.5	200.8	54.8	**4.704**	**0.099**
MG-138A_07	0.00408	0.00067	0.00060	0.00000	0.10725	0.00760	0.01075	14.3	0.00074	1.7	0.12	0.10606	14.2	10.9	1.5	4.7	0.1	1732.5	260.3	56.4	**4.738**	**0.082**
MG-138A_19	0.00180	0.00140	0.00060	0.00001	0.07652	0.00560	0.00770	14.8	0.00074	2.2	0.15	0.07567	14.7	7.8	1.1	4.8	0.1	1086.0	293.8	38.9	**4.753**	**0.104**
MG-138A_08	0.00699	0.00010	0.00061	0.00000	0.08362	0.00079	0.00846	2.3	0.00074	1.1	0.47	0.08268	2.0	8.5	0.2	4.8	0.1	1261.5	39.4	44.1	**4.780**	**0.052**
MG-138A_05	0.00680	0.00075	0.00061	0.00000	0.07775	0.00270	0.00795	7.2	0.00075	1.7	0.23	0.07688	7.0	8.0	0.6	4.8	0.1	1118.0	139.3	39.9	**4.836**	**0.081**
MG-138A_13	0.00823	0.00046	0.00062	0.00001	0.09786	0.00350	0.01010	7.4	0.00076	1.9	0.26	0.09677	7.2	10.2	0.8	4.9	0.1	1562.5	134.8	52.2	**4.878**	**0.094**
MG-138A_18	0.01234	0.00064	0.00062	0.00001	0.11657	0.00430	0.01206	7.7	0.00076	2.1	0.27	0.11527	7.4	12.2	0.9	4.9	0.1	1884.0	133.5	59.8	**4.889**	**0.101**
MG-138A_04	0.00262	0.00074	0.00063	0.00001	0.11310	0.00760	0.01187	13.9	0.00077	3.6	0.26	0.11184	13.5	12.0	1.7	5.0	0.2	1829.5	243.9	58.6	**4.960**	**0.178**
MG-138A_33	0.00643	0.00095	0.00063	0.00001	0.11128	0.00520	0.01177	9.6	0.00078	2.2	0.23	0.11004	9.4	11.9	1.1	5.0	0.1	1800.0	170.5	57.9	**5.001**	**0.110**
MG-138A_32	0.00601	0.00110	0.00066	0.00001	0.08334	0.00580	0.00917	14.2	0.00081	2.5	0.18	0.08241	13.9	9.3	1.3	5.2	0.1	1255.0	272.6	43.9	**5.199**	**0.131**
MG-138A_01	0.00366	0.00084	0.00066	0.00001	0.18284	0.00920	0.02024	10.7	0.00081	3.4	0.32	0.18080	10.1	20.3	2.1	5.2	0.2	2660.0	167.2	74.3	**5.231**	**0.179**
MG-138A_06	-0.00002	0.00058	0.00066	0.00001	0.13957	0.00780	0.01546	11.8	0.00081	3.7	0.31	0.13801	11.2	15.6	1.8	5.2	0.2	2202.0	194.5	66.4	**5.236**	**0.194**
MG-138A_02	0.00200	0.00190	0.00069	0.00001	0.17845	0.00930	0.02049	11.0	0.00084	3.6	0.33	0.17645	10.4	20.6	2.3	5.4	0.2	2619.5	173.8	73.6	**5.427**	**0.194**
MG-138A_40	0.02349	0.00140	0.00077	0.00001	0.21197	0.00550	0.02741	5.7	0.00095	2.2	0.38	0.20960	5.2	27.5	1.5	6.1	0.1	2902.0	84.9	77.7	**6.111**	**0.133**
MG-138A_34	0.00453	0.00190	0.00088	0.00002	0.20828	0.01100	0.03048	11.3	0.00107	4.0	0.35	0.20595	10.6	30.5	3.4	6.9	0.3	2873.5	172.1	77.3	**6.915**	**0.274**
MG-138A_23	0.02351	0.00089	0.00109	0.00001	0.12278	0.00160	0.02244	3.0	0.00134	1.3	0.42	0.12141	2.7	22.5	0.7	8.6	0.1	1977.0	48.1	61.7	**8.637**	**0.109**
MG-138A_03	0.01373	0.00290	0.00111	0.00005	0.37077	0.01100	0.06886	11.1	0.00136	9.4	0.84	0.36662	6.0	67.6	7.3	8.8	0.8	3777.5	90.6	87.0	**8.775**	**0.823**
MG-138A_24	0.00954	0.00012	0.00114	0.00000	0.05425	0.00049	0.01033	2.2	0.00140	1.0	0.45	0.05364	1.9	10.4	0.2	9.0	0.1	355.5	43.8	13.8	**8.999**	**0.088**
MG-138A_35	0.00887	0.00016	0.00117	0.00000	0.05155	0.00063	0.01004	2.8	0.00143	1.1	0.38	0.05097	2.5	10.1	0.3	9.2	0.1	239.5	58.7	9.3	**9.199**	**0.097**
MG-138A_11	0.01130	0.00110	0.00117	0.00001	0.05691	0.00140	0.01114	5.2	0.00144	1.6	0.31	0.05628	5.0	11.2	0.6	9.2	0.1	463.0	110.2	17.8	**9.246**	**0.148**
MG-138A_25	0.02288	0.00083	0.00122	0.00000	0.10413	0.00170	0.02124	3.5	0.00150	1.1	0.32	0.10297	3.3	21.3	0.7	9.6	0.1	1678.0	61.7	54.8	**9.635**	**0.109**
MG-138A_30	0.00863	0.00014	0.00128	0.00000	0.04724	0.00046	0.01012	2.3	0.00157	1.0	0.45	0.04672	2.1	10.2	0.2	10.1	0.1	34.5	49.6	1.0	**10.122**	**0.105**
MG-138A_37	0.03910	0.00120	0.00136	0.00001	0.19668	0.00280	0.04474	3.3	0.00167	1.4	0.43	0.19448	2.9	44.4	1.4	10.7	0.2	2780.0	48.1	75.8	**10.746**	**0.150**
MG-138A_10	0.04877	0.00650	0.00167	0.00004	0.31530	0.00920	0.08770	7.3	0.00204	4.3	0.59	0.31178	5.9	85.3	5.9	13.1	0.6	3529.5	90.7	84.6	**13.137**	**0.562**
MG-138A_09	0.01823	0.00130	0.00225	0.00001	0.05157	0.00089	0.01940	3.7	0.00276	1.2	0.32	0.05100	3.5	19.5	0.7	17.8	0.2	240.5	81.2	9.0	**17.763**	**0.213**
MG-138A_21	0.02185	0.00051	0.00278	0.00001	0.04640	0.00039	0.02158	2.1	0.00341	1.0	0.50	0.04588	1.8	21.7	0.5	21.9	0.2	#N/A	#N/A	-1.3	**21.949**	**0.229**
MG-138A_27	0.06965	0.00160	0.00892	0.00003	0.05364	0.00042	0.07990	2.0	0.01093	1.1	0.53	0.05304	1.7	78.1	1.5	70.0	0.8	330.5	39.0	10.3	**70.047**	**0.752**
MG-138A_17	0.07791	0.00150	0.01056	0.00003	0.04898	0.00016	0.08639	1.4	0.01294	1.0	0.72	0.04843	1.0	84.1	1.1	82.9	0.8	120.0	22.7	1.5	**82.870**	**0.821**
MG-138A_12	0.08413	0.00085	0.01236	0.00003	0.04861	0.00010	0.10034	1.3	0.01514	0.9	0.76	0.04806	0.8	97.1	1.2	96.9	0.9	102.0	19.3	0.2	**96.874**	**0.913**
MG-138A_14	0.11347	0.00240	0.01662	0.00005	0.04969	0.00021	0.13795	1.5	0.02036	1.0	0.67	0.04914	1.1	131.2	1.8	129.9	1.3	154.0	25.8	1.0	**129.940**	**1.284**
MG-138A_26	0.12290	0.00140	0.01688	0.00005	0.04931	0.00010	0.13902	1.3	0.02068	1.0	0.77	0.04876	0.8	132.2	1.6	131.9	1.3	136.0	19.2	0.2	**131.931**	**1.288**
MG-138A_38	0.09167	0.00690	0.01699	0.00005	0.05070	0.00025	0.14388	1.6	0.02081	1.0	0.64	0.05014	1.2	136.5	2.0	132.8	1.3	201.0	28.2	2.7	**132.791**	**1.321**
MG-138A_28	0.11321	0.00820	0.01705	0.00005	0.05448	0.00051	0.15516	2.2	0.02089	1.0	0.45	0.05387	2.0	146.4	3.0	133.3	1.3	365.5	45.1	9.0	**133.263**	**1.314**
MG-138A_31	0.11564	0.00730	0.01766	0.00006	0.05039	0.00034	0.14863	1.8	0.02163	1.0	0.57	0.04983	1.5	140.7	2.4	138.0	1.4	186.5	35.5	1.9	**137.975**	**1.429**
MG-138A_22	0.13096	0.00200	0.01784	0.00005	0.04919	0.00011	0.14657	1.3	0.02185	1.0	0.77	0.04864	0.8	138.9	1.7	139.4	1.4	130.5	19.7	-0.3	**139.354**	**1.389**
MG-138A_36	0.12344	0.00240	0.01856	0.00008	0.04994	0.00016	0.15478	1.5	0.02273	1.1	0.77	0.04939	1.0	146.1	2.0	144.9	1.6	166.0	22.3	0.8	**144.880**	**1.635**
MG-138A_29	2.08968	0.06600	0.16022	0.00041	0.08164	0.00006	2.18438	1.2	0.19624	1.0	0.80	0.08073	0.7	1176.0	8.3	1155.1	10.1	1214.5	14.2	1.8	**1155.064**	**10.091**
MG-138A_39	8.73260	0.17000	0.34361	0.00110	0.16764	0.00007	9.61895	1.3	0.42086	1.0	0.82	0.16576	0.7	2398.9	11.5	2264.3	19.6	2515.0	12.0	5.6	**2264.313**	**19.637**

Supplementary References

ACOREMA, 2018. Mamíferos marinos de la Provincia de Pisco.

Acosta-Hospitaleche, C., Altamirano-Sierra, A. and Stucchi, M., 2011. Variaciones morfológicas del tarsometatarso de los pingüinos (Aves, Sphenisciformes) de la secuencia estratigráfica de la Formación Pisco (Mioceno-Plioceno), Perú. Revista Mexicana de Ciencias Geológicas, 28: 290-300.

Altamirano-Sierra, A., 2014. Tiburones de la provincia de Pisco.

Altamirano-Sierra, A.J., 2013. Primer registro de pelícano (Aves: Pelecanidae) para el Mioceno tardío de la formación Pisco, Perú. Bulletin de l'Institut français d'études andines, 42(1).

Amson, E., Billet, G. and Muizon, C.d., 2018. Evolutionary adaptation to aquatic lifestyle in extinct sloths can lead to systemic alteration of bone structure. Proceedings of the Royal Society B: Biological Sciences, 285(1878): 20180270. https://doi.org/10.1098/rspb.2018.0270

Amson, E. and Muizon, C.d., 2013. A new durophagous phocid (Mammalia: Carnivora) from the late Neogene of Peru and considerations on monachine seals phylogeny. Journal of Systematic Palaeontology, 12(5): 523-548. https://doi.org/10.1080/14772019.2013.799610

Amson, E. and Muizon, C.d., 2014. A new durophagous phocid (Mammalia: Carnivora) from the late Neogene of Peru and considerations on monachine seals phylogeny. Journal of Systematic Palaeontology, 12(5): 523-548.

Amson, E., Muizon, C.d., Domning, D.P., Argot, C. and De Buffrénil, V., 2015. Bone histology as a clue for resolving the puzzle of a dugong rib in the Pisco Formation, Peru. Journal of Vertebrate Paleontology, 35(3): e922981. https://doi.org/10.1080/02724634.2014.922981

Amson, E., Muizon, C.d., Laurin, M., Argot, C. and de Buffrénil, V., 2014. Gradual adaptation of bone structure to aquatic lifestyle in extinct sloths from Peru. Proceedings of the Royal Society B: Biological Sciences, 281(1782): 20140192. https://doi.org/10.1098/rspb.2014.0192

Barron, J.A., 2003. Planktonic marine diatom record of the past 18 my: appearances and extinctions in the Pacific and Southern Oceans. Diatom Research, 18(2): 203-224.

Benites-Palomino, A., Velez-Juarbe, J., Collareta, A., Ochoa, D., Altamirano, A., Carré, M., Laime, M., Urbina, M. and Salas-Gismondi, R., in press. Nasal compartmentalization in Kogiidae (Cetacea, Physeteroidea): Insights from a new late Miocene dwarf sperm whale from the Pisco Formation. Papers in Palaeontology.

Benites-Palomino, A., Velez-Juarbe, J., Salas-Gismondi, R. and Urbina, M., 2020. *Scaphokogia totajpe*, sp. nov., a new bulky-faced pygmy sperm whale (Kogiidae) from the late Miocene of Peru. Journal of Vertebrate Paleontology, e1728538. https://doi.org/10.1080/02724634.2019.1728538

Berta, A., Churchill, M. and Boessenecker, R.W., 2018. The origin and evolutionary biology of pinnipeds: seals, sea lions, and walruses. Annual Review of Earth and Planetary Sciences, 46: 203-228. https://doi.org/10.1146/annurev-earth-082517-010009

Berta, A. and Deméré, T.A., 1986. *Callorhinus gilmorei* n. sp.,(Carnivora: Otariidae) from the San Diego Formation (Blancan) and its implications for otariid phylogeny. San Diego Society of Natural History, pp. 111-126.

Bianucci, G., Claudio, D.C., Landini, W., Klaas, P., Tinelli, C., Christian, d.M., Gariboldi, K., Elisa, M., Gino, C. and Gioncada, A., 2015. Fossil Marine Vertebrate in Cerro Colorado. The type locality of the giant raptorial Livyatan melvillei (Miocene, Pisco formation, Peru).

Bianucci, G., Collareta, A., Bosio, G., Landini, W., Gariboldi, K., Gioncada, A., Lambert, O., Malinverno, E., Muizon, C.d., Varas-Malca, R., Villa, I., Coletti, G., Urbina, M. and Di Celma, C., 2018. Taphonomy and palaeoecology of the lower Miocene marine vertebrate assemblage of Ullujaya (Chilcatay Formation, East Pisco Basin, southern Peru). Palaeogeography, Palaeoclimatology, Palaeoecology, 511: 256-279. https://doi.org/10.1016/j.palaeo.2018.08.013

Bianucci, G., Di Celma, C., Collareta, A., Landini, W., Post, K., Tinelli, C., Muizon, C.d., Bosio, G., Gariboldi, K. and Gioncada, A., 2016a. Fossil marine vertebrates of Cerro Los Quesos: Distribution of cetaceans, seals, crocodiles, seabirds, sharks, and bony fish in a late Miocene locality of the Pisco Basin, Peru. Journal of Maps, 12(5): 1037-1046. https://doi.org/10.1080/17445647.2015.1115785

Bianucci, G., Di Celma, C., Landini, W., Post, K., Tinelli, C., Muizon, C.d., Gariboldi, K., Malinverno, E., Cantalamessa, G. and Gioncada, A., 2016b. Distribution of fossil marine vertebrates in Cerro Colorado, the type locality of the giant raptorial sperm whale Livyatan melvillei (Miocene, Pisco Formation, Peru). Journal of Maps, 12(3): 543-557. https://doi.org/10.1080/17445647.2015.1048315

Bianucci, G., Lambert, O. and Post, K., 2010. High concentration of long-snouted beaked whales (genus Messapicetus) from the Miocene of Peru. Palaeontology, 53(5): 1077-1098.

Bianucci, G., Muizon, C.d., Urbina, M. and Lambert, O., 2020. Extensive Diversity and Disparity of the Early Miocene Platanistoids (Cetacea, Odontoceti) in the Southeastern Pacific (Chilcatay Formation, Peru). Life, 10(3): 27. https://doi.org/10.3390/life10030027

Bianucci, G., Sorbi, S., Suárez, M.E. and Landini, W., 2006. The southernmost sirenian record in the eastern Pacific Ocean, from the Late Miocene of Chile. Comptes Rendus Palevol, 5(8): 945-952.

BirdLife Intenational, 2020. https://www.birdlife.org/americas

Bisconti, M., 2012. Comparative osteology and phylogenetic relationships of Miocaperea pulchra, the first fossil pygmy right whale genus and species (Cetacea, Mysticeti, Neobalaenidae). Zoological Journal of the Linnean Society, 166(4): 876-911.

Black, L.P., Kamo, S.L., Allen, C.M., Davis, D.W., Aleinikoff, J.N., Valley, J.W., Mundil, R., Campbell, I.H., Korsch, R.J. and Williams, I.S., 2004. Improved 206Pb/238U microprobe geochronology by the monitoring of a trace-element-related matrix effect; SHRIMP, ID–TIMS, ELA–ICP–MS and oxygen isotope documentation for a series of zircon standards. Chemical Geology, 205(1-2): 115-140.

Bosio, G., Malinverno, E., Collareta, A., Di Celma, C., Gioncada, A., Parente, M., Berra, F., Marx, F.G., Vertino, A. and Urbina, M., 2020. Strontium Isotope Stratigraphy and the thermophilic fossil fauna from the middle Miocene of the East Pisco Basin (Peru). Journal of South American Earth Sciences, 97: 102399. https://doi.org/10.1016/j.jsames.2019.102399

Bosio, G., Malinverno, E., Villa, I., Di Celma, C., Gariboldi, K., Gioncada, A., Barberini, V., Urbina, M. and Bianucci, G., 2019. Tephrochronology and chronostratigraphy of the Miocene Chilcatay and Pisco formations (East Pisco Basin, Peru). Newsletters on Stratigraphy, 53(2): 213-247. https://doi.org/10.1127/NOS%2F2019%2F0525

Bouetel, V. and Muizon, C.d., 2006. The anatomy and relationships of *Piscobalaena nana* (Cetacea, Mysticeti), a Cetotheriidae ss from the early Pliocene of Peru. Geodiversitas, 28(2): 319-395.

Brand, L., Urbina, M., Chadwick, A., DeVries, T.J. and Esperante, R., 2011. A high resolution stratigraphic framework for the remarkable fossil cetacean assemblage of the Miocene/Pliocene Pisco Formation, Peru. Journal of South American Earth Sciences, 31(4): 414-425. https://doi.org/10.1016/j.jsames.2011.02.015

Chao, A., Colwell, R.K., Lin, C.-W. and Gotelli, N.J., 2009. Sufficient sampling for asymptotic minimum species richness estimators. Ecology, 90(4): 1125-1133. https://doi.org/10.1890/07-2147.1

Chao, A., Ma, K., Hsieh, T. and Chiu, C.-H., 2016. User’s guide for online program SpadeR (Species-richness prediction and diversity estimation in R). National Tsing Hua University, Taiwan: 88.

Chavez, M., Stucchi, M. and Urbina, M., 2007. El registro de Pelagornithidae (Aves: Pelecaniformes) y la avifauna neógena del Pacífico sudeste. Bulletin de l'Institut français d'études andines, 36(2): 175-197.

Cheneval, J., 1993. L'avifaune Mio-Pliocène de la Formation Pisco (Pérou): étude préliminaire. Documents des laboratoires de géologie (Lyon), 125: 85-95.

Chiu, C.H., Wang, Y.T., Walther, B.A. and Chao, A., 2014. An improved nonparametric lower bound of species richness via a modified Good–Turing frequency formula. Biometrics, 70(3): 671-682. https://doi.org/10.1111/biom.12200

Churchill, M., Boessenecker, R.W. and Clementz, M.T., 2014. Colonization of the Southern Hemisphere by fur seals and sea lions (Carnivora: Otariidae) revealed by combined evidence phylogenetic and Bayesian biogeographical analysis. Zoological Journal of the Linnean Society, 172(1): 200-225. https://doi.org/10.1111/zoj.12163

Colbert, E.H., 1944. A new fossil whale from the Miocene of Peru, 83. American Museum of Natural History, 32 pp.

Collareta, A., Lambert, O., Muizon, C.d., Urbina, M. and Bianucci, G., 2017. *Koristocetus pescei* gen. et sp. nov., a diminutive sperm whale (Cetacea: Odontoceti: Kogiidae) from the late Miocene of Peru. Fossil Record, 20: 259-278. https://doi.org/10.5194/fr-20-259-2017

Cornejo, R., Vélez-Zuazo, X., González-Pestana, A., Kouri, C. and Mucientes, G., 2015. An updated checklist of Chondrichthyes from the southeast Pacific off Peru. Check List, 11(6): 1809. https://doi.org/10.15560/11.6.1809

Deméré, T.A., Berta, A. and Adam, P., 2003. Chapter 3: Pinnipedimorph evolutionary biogeography. Bulletin of the American Museum of Natural History, 279: 32-76. https://doi.org/10.1206/0003-0090(2003)279<0032:C>2.0.CO;2

DeVries, T.J., 1998. Oligocene deposition and Cenozoic sequence boundaries in the Pisco Basin (Peru). Journal of South American Earth Sciences, 11(3): 217-231. https://doi.org/10.1016/S0895-9811(98)00014-5

DeVries, T.J., 2002. Patterns of diversity in Cenozoic marine mollusks from the Peruvian province, Geol. Soc. Am. Abstr. Progr., pp. 39.

DeVries, T.J., 2020. Lithostratigraphy and Biostratigraphy of Pliocene and Pleistocene Marine Deposits and Age of the highest Marine Terrace from the Sacaco Basin and its Environs (southern Peru). Boletín de la Sociedad Geológica del Perú, in press.

DeVries, T.J. and Jud, N., 2018. Lithofacies patterns and paleogeography of the Miocene Chilcatay and lower Pisco depositional sequences (East Pisco Basin, Peru). Boletín de la Sociedad Geológica del Perú, volumen jubilar, 8: 124-167.

Di Celma, C., Malinverno, E., Bosio, G., Collareta, A., Gariboldi, K., Gioncada, A., Molli, G., Basso, D., Varas-Malca, R.M. and Pierantoni, P.P., 2017. Sequence stratigraphy and paleontology of the Upper Miocene Pisco Formation along the western side of the lower Ica Valley (Ica Desert, Peru). Riv Ital Paleontol Stratigr, 123: 255-273. https://doi.org/10.13130/2039-4942/8373

Di Celma, C., Malinverno, E., Cantalamessa, G., Gioncada, A., Bosio, G., Villa, I.M., Gariboldi, K., Rustichelli, A., Pierantoni, P. and Landini, W., 2016. Stratigraphic framework of the late Miocene Pisco Formation at Cerro Los Quesos (Ica Desert, Peru). Journal of maps, 12(5): 1020-1028. https://doi.org/10.1080/17445647.2015.1115783

Di Celma, C., Malinverno, E., Collareta, A., Bosio, G., Gariboldi, K., Lambert, O., Landini, W., Pierantoni, P., Gioncada, A. and Villa, I., 2018. Facies analysis, stratigraphy and marine vertebrate assemblage of the lower Miocene Chilcatay Formation at Ullujaya (Pisco basin, Peru). Journal of Maps, 14(2): 257-268. https://doi.org/10.1080/17445647.2018.1456490

Di Celma, C., Pierantoni, P., Malinverno, E., Collareta, A., Lambert, O., Landini, W., Bosio, G., Gariboldi, K., Gioncada, A. and Muizon, C.d., 2019. Allostratigraphy and paleontology of the lower Miocene Chilcatay Formation in the Zamaca area, East Pisco basin, southern Peru. Journal of Maps, 15(2): 393-405.

Domning, D.P., 2001. The earliest known fully quadrupedal sirenian. Nature, 413(6856): 625-627. https://doi.org/10.1038/35098072

Domning, D.P. and Aguilera, O.A., 2008. Fossil Sirenia of the West Atlantic and Caribbean region. VIII. Nanosiren garciae, gen. et sp. nov. and Nanosiren sanchezi, sp. nov. Journal of Vertebrate Paleontology, 28(2): 479-500. https://doi.org/10.1671/0272-4634(2008)28[479:FSOTWA]2.0.CO;2

Dunbar, R.B., Marty, R.C. and Baker, P.A., 1990. Cenozoic marine sedimentation in the Sechura and Pisco basins, Peru. Palaeogeography, Palaeoclimatology, Palaeoecology, 77(3): 235-261. https://doi.org/10.1016/0031-0182(90)90179-B

Ehret, D.J., Macfadden, B.J., Jones, D.S., DeVries, T.J., Foster, D.A. and Salas-Gismondi, R., 2012. Origin of the white shark Carcharodon (Lamniformes: Lamnidae) based on recalibration of the Upper Neogene Pisco Formation of Peru. Palaeontology, 55(6): 1139-1153. https://doi.org/10.1111/j.1475-4983.2012.01201.x

Esperante, R., Brand, L.R., Chadwick, A.V. and Poma, O., 2015. Taphonomy and paleoenvironmental conditions of deposition of fossil whales in the diatomaceous sediments of the Miocene/Pliocene Pisco Formation, southern Peru—A new fossil-lagerstätte. Palaeogeography, Palaeoclimatology, Palaeoecology, 417: 337-370. https://doi.org/10.1016/j.palaeo.2014.09.029

Foote, M., 2000. Deep time: Paleobiology's perspective. Paleobiology, 26(Suppl. to No. 4): 74-102.

Gariboldi, K., Bosio, G., Malinverno, E., Gioncada, A., Di Celma, C., Villa, I.M., Urbina, M. and Bianucci, G., 2017. Biostratigraphy, geochronology and sedimentation rates of the upper Miocene Pisco Formation at two important marine vertebrate fossil-bearing sites of southern Peru. Newsletters on Stratigraphy, 50(4): 417-444. https://doi.org/10.1127/nos/2017/0345

Göhlich, U., 2007. The oldest fossil record of the extant penguin genus Spheniscus-a new species from the Miocene of Peru. Acta Palaeontologica Polonica, 52(2).

Gutstein, C.S., Cozzuol, M.A., Vargas, A.O., Suárez, M.E., Schultz, C.L. and Rubilar-Rogers, D., 2009. Patterns of skull variation of Brachydelphis (Cetacea, Odontoceti) from the Neogene of the Southeastern Pacific. Journal of Mammalogy, 90(2): 504-519. https://doi.org/10.1644/07-MAMM-A-081.1

Hospitaleche-Acosta, C. and Stucchi, M., 2005. Nuevos restos terciarios de Spheniscidae (Aves, Sphenisciformes) procedentes de la costa del Perú. Revista Española de Paleontología, 20(1): 1-5.

Kelez, S., van Oordt, F., de Paz, N. and Forsberg, K., 2005. Simposio de Tortugas Marinas en el Pacífico Sur Oriental.

Kraus, R., 1998. The cranium of *Piscogavialis jugaliperforatus* n. gen., n. sp.(Gavialidae, Crocodylia) from the Miocene of Peru. Paläontologische Zeitschrift, 72(3-4): 389-405. https://doi.org/10.1007/BF02988368

Lambert, O., Bianucci, G. and Beatty, B.L., 2014. Bony outgrowths on the jaws of an extinct sperm whale support macroraptorial feeding in several stem physeteroids. Naturwissenschaften, 101(6): 517-521. https://doi.org/10.1007/s00114-014-1182-2

Lambert, O., Bianucci, G. and Muizon, C.d., 2016. Macroraptorial sperm whales (Cetacea, Odontoceti, Physeteroidea) from the Miocene of Peru. Zoological Journal of the Linnean Society, 179(2): 404-474. https://doi.org/10.1111/zoj.12456

Lambert, O., Bianucci, G. and Post, K., 2009. A new beaked whale (Odontoceti, Ziphiidae) from the middle Miocene of Peru. Journal of Vertebrate Paleontology, 29(3): 910-922. https://doi.org/10.1671/039.029.0304

Lambert, O., Bianucci, G., Post, K., Muizon, C.d., Salas-Gismondi, R., Urbina, M. and Reumer, J., 2010. The giant bite of a new raptorial sperm whale from the Miocene epoch of Peru. Nature, 466(7302): 105. https://doi.org/10.1038/nature09067

Lambert, O., Bianucci, G., Urbina, M. and Geisler, J.H., 2017. A new inioid (Cetacea, Odontoceti, Delphinida) from the Miocene of Peru and the origin of modern dolphin and porpoise families. Zoological Journal of the Linnean Society, 179(4): 919-946. https://doi.org/10.1111/zoj.12479

Lambert, O., Collareta, A., Benites-Palomino, A., Di Celma, C., Muizon, C.d., Urbina, M. and Bianucci, G., 2020. A new small, mesorostrine inioid (Ctacea, Odontoceti, Delphinida) from four late Miocene localities of the Pisco Formation. Papers in Palaeontology: 1-22. https://doi.org/10.1002/spp2.1332

Lambert, O., Collareta, A., Landini, W., Post, K., Ramassamy, B., Di Celma, C., Urbina, M. and Bianucci, G., 2015. No deep diving: evidence of predation on epipelagic fish for a stem beaked whale from the Late Miocene of Peru. Proceedings of the Royal Society Biological Sciences, 282(1815): 20151530. https://doi.org/10.1098/rspb.2015.1530

Lambert, O. and Muizon, C.d., 2013. A new long-snouted species of the Miocene pontoporiid dolphin Brachydelphis and a review of the Mio-Pliocene marine mammal levels in the Sacaco Basin, Peru. Journal of Vertebrate Paleontology, 33(3): 709-721. https://doi.org/10.1080/02724634.2013.743405

Lambert, O., Muizon, C.d. and Bianucci, G., 2013. The most basal beaked whale Ninoziphius platyrostris Muizon, 1983: clues on the evolutionary history of the family Ziphiidae (Cetacea: Odontoceti). Zoological Journal of the Linnean Society, 167(4): 569-598. https://doi.org/10.1111/zoj.12018

Landini, W., Altamirano-Sierra, A., Collareta, A., Di Celma, C., Urbina, M. and Bianucci, G., 2017. The late Miocene elasmobranch assemblage from Cerro Colorado (Pisco Formation, Peru). Journal of South American Earth Sciences, 73: 168-190. https://doi.org/10.1016/j.jsames.2016.12.010

Landini, W., Collareta, A., Di Celma, C., Malinverno, E., Urbina, M. and Bianucci, G., 2019. The early miocene elasmobranch assemblage from Zamaca (Chilcatay formation, Peru). Journal of South American Earth Sciences, 91: 352-371. https://doi.org/10.1016/j.jsames.2018.08.004

Marx, F.G. and Kohno, N., 2016. A new Miocene baleen whale from the Peruvian desert. Royal Society Open Science, 3(10): 160542.

Marx, F.G., Lambert, O. and Muizon, C.d., 2017. A new Miocene baleen whale from Peru deciphers the dawn of cetotheriids. Royal Society Open Science, 4(9): 170560. https://doi.org/doi:10.1098/rsos.170560

McArthur, J., Howarth, R. and Shields, G., 2012. Strontium isotope stratigraphy. The geologic time scale, 1: 127-144. https://doi.org/10.1016/B978-0-444-59425-9.00007-X

Mcdonald, H.G. and Muizon, C.d., 2002. The cranial anatomy of Thalassocnus (Xenarthra, Mammalia), a derived nothrothere from the Neogene of the Pisco Formation (Peru). Journal of Vertebrate Paleontology, 22(2): 349-365. https://doi.org/10.1671/0272-4634(2002)022%5B0349:TCAOTX%5D2.0.CO;2

Muizon, C.d., 1978. Arctocephalus (Hydrarctos) lomasiensis, subgen, nov. et nov. sp., un nouvel Otariidae du Mio-Pliocene de Sacaco (Perou). Bulletin de l'Institut Francais des Etudes Andines, 7(3-4): 169-188.

Muizon, C.d., 1981. Les vertébrés fossiles de la formation Pisco (Pérou), 22. Éditions ADPF.

Muizon, C.d., 1984. Un Ziphiidae (Cetacea) nouveau du Pliocène inférieur du Pérou. Comptes-rendus des séances de l'Académie des sciences. Série 2, Mécanique-physique, chimie, sciences de l'univers, sciences de la terre, 297(1): 85-88.

Muizon, C.d., 1988. Les relations phylogenetiques des Delphinida (Cetacea, mammalia). Annales de paléontologie 74(4): 159-227.

Muizon, C.d., 1993. Walrus-like feeding adaptation in a new cetacean from the Pliocene of Peru. Nature, 365(6448): 745-748.

Muizon, C.d. and Bellon, H., 1980. L'âge mio-pliocène de la Formation Pisco (Pérou). Comptes Rendus hebdomadaires des Séances de l'Académie des Sciences, Paris, série D, 290: 1063-1066.

Muizon, C.d. and Bellon, H., 1986. Nouvelles données sur l'âge de la Formation Pisco (Pérou). Comptes rendus de l'Académie des sciences. Série 2, Mécanique, Physique, Chimie, Sciences de l'univers, Sciences de la Terre, 303(15): 1401-1404.

Muizon, C.d. and DeVries, T.J., 1985. Geology and paleontology of late Cenozoic marine deposits in the Sacaco area (Peru). Geologische Rundschau, 74(3): 547-563. https://doi.org/10.1007/BF01821211

Muizon, C.d. and Domning, D., 1985. The first records of fossil sirenians in the southeastern Pacific Ocean. Bulletin du Muséum national d'histoire naturelle. Section C, Sciences de la terre, paléontologie, géologie, minéralogie, 7(3): 189-213.

Muizon, C.d. and Domning, D.P., 2002. The anatomy of Odobenocetops (Delphinoidea, Mammalia), the walrus-like dolphin from the Pliocene of Peru and its palaeobiological implications. Zoological Journal of the Linnean Society, 134(4): 423-452. https://doi.org/10.1046/j.1096-3642.2002.00015.x

Muizon, C.d. and McDonald, H., 1995. An aquatic sloth from the Pliocene of Peru. Nature, 375(6528): 224-227.

Muizon, C.d., Mcdonald, H.G., Salas-Gismondi, R. and Urbina, M., 2003. A new early species of the aquatic sloth Thalassocnus (Mammalia, Xenarthra) from the Late Miocene of Peru. Journal of Vertebrate Paleontology, 23(4): 886-894. https://doi.org/10.1671/2361-13

Muizon, C.d., McDonald, H.G., Salas-Gismondi, R. and Urbina, M., 2004a. The evolution of feeding adaptations of the aquatic sloth Thalassocnus. Journal of Vertebrate Paleontology, 24(2): 398-410. https://doi.org/10.1671/2429b

Muizon, C.d., McDonald, H.G., Salas-Gismondi, R. and Urbina, M., 2004b. The youngest species of the aquatic sloth Thalassocnus and a reassessment of the relationships of the nothrothere sloths (Mammalia: Xenarthra). Journal of Vertebrate Paleontology, 24(2): 387-397. https://doi.org/10.1671/2429a

O'Hare, D.J., 2015. High-Resolution Correlation of a Time-Bounded Unit of the Pisco Formation, Peru. Master Thesis, Loma Linda University, Electronic Theses, Dissertations & Projects. Paper 333, 170 pp.

Parham, J.F. and Pyenson, N.D., 2010. New sea turtle from the Miocene of Peru and the iterative evolution of feeding ecomorphologies since the Cretaceous. Journal of Paleontology, 84(2): 231-247. https://doi.org/10.1666/09-077R.1

Pilleri, G. and Pilleri, O., 1989. Balaenoptera siberi, ein neuer balaenopterid (Cetacea) aus der Pisco-Formation Perus I. Beitrage zur Palaeontologie der Cetaceen Perus I: 63-106.

Pilleri, G. and Siber, H., 1989. Neuer spättertiärer cetotherid (Cetacea, Mysticeti) aus der Pisco Formation Perus. Beiträge zur Paläontologie der Cetaceen Perus, 1: 108-122.

R-Core Team, 2018. R: A language and environment for statistical computing, R Foundation for Statistical Computing. URL http://www.r-project.org/, Vienna, Austria.

Salas-Gismondi, R., Flynn, J.J., Baby, P., Tejada-Lara, J.V., Claude, J. and Antoine, P.-O., 2016. A new 13 million year old gavialoid crocodylian from proto-Amazonian mega-wetlands reveals parallel evolutionary trends in skull shape linked to longirostry. PloS one, 11(4). https://doi.org/10.1371/journal.pone.0152453

Salas-Gismondi, R., Moreno-Bernal, J.W., Scheyer, T.M., Sánchez-Villagra, M.R. and Jaramillo, C., 2019. New Miocene Caribbean gavialoids and patterns of longirostry in crocodylians. Journal of Systematic Palaeontology, 17(12): 1049-1075. https://doi.org/10.1080/14772019.2018.1495275

Stucchi, M., 2002. Una nueva especie de Spheniscus (Aves: Spheniscidae) de la formación Pisco, Perú. Boletín de la Sociedad Geológica del Perú, 94: 17-24. https://doi.org/10.4000/bifea.6488

Stucchi, M., 2007. Los pingüinos de la formación Pisco (Neógeno), Perú, 4th European Meeting on the Palaeontology and Stratigraphy of Latin America Cuadernos del Museo Geominero. Instituto Geológico y Minero de España; Madrid, pp. 367-373.

Stucchi, M., 2008. Reporte preliminar de un cráneo de Pelagornithidae (Aves: Odontopterigyformes) de la base de la formación Pisco, Perú (Mioceno medio). Lima, diciembre de 2008. Bulletin de l'Institut français d'études andines(37 (3)): 580-582. https://doi.org/10.4000/bifea.3073

Stucchi, M. and DeVries, T.J., 2003. El registro más antiguo de Sulidae (Aves) en el Perú. Boletín de la Sociedad Geológica del Perú, 96: 95-98.

Stucchi, M. and Emslie, S.D., 2005. A new condor (Ciconiiformes, Vulturidae) from the late Miocene/early Pliocene Pisco formation, Peru. The Condor, 107(1): 107-113. https://doi.org/10.1650/7475

Stucchi, M., Emslie, S.D., Varas-Malca, R.M. and Urbina-Schmitt, M., 2015a. A new Late Miocene condor (Aves, Cathartidae) from Peru and the origin of South American condors. Journal of Vertebrate Paleontology, 35(5): e972507. https://doi.org/10.1080/02724634.2015.972507

Stucchi, M. and Urbina, M., 2004. Ramphastosula (Aves, Sulidae): a new genus from the early Pliocene of the Pisco Formation, Peru. Journal of Vertebrate Paleontology, 24(4): 974-978. https://doi.org/10.1671/0272-4634(2004)024[0974:RASANG]2.0.CO;2

Stucchi, M. and Urbina, M., 2005. Nuevos restos de Procellariiformes (Aves) de la Formacion Pisco, Peru. Boletín de la Sociedad geológica del Perú, 100: 67-77.

Stucchi, M., Urbina, M. and Giraldo, A., 2003. Una nueva especie de Spheniscidae del Mioceno tardío de la Formación Pisco, Perú. Bulletin de l'Institut français d'études andines(32 (2)): 361-375. https://doi.org/10.4000/bifea.6541

Stucchi, M., Varas-Malca, R.M. and Urbina-Schmitt, M., 2015b. New Miocene sulid birds from Peru and considerations on their Neogene fossil record in the Eastern Pacific Ocean. Acta Palaeontologica Polonica, 61(2): 417-427.

Stucchi, M., Varas-Malca, R.M. and Urbina-Schmitt, M., 2016. New Miocene sulid birds from Peru and considerations on their Neogene fossil record in the Eastern Pacific Ocean. Acta Palaeontologica Polonica, 61(2): 417-428. https://doi.org/10.4202/app.00170.2015

Tarquini, J., Morgan, C.C., Toledo, N. and Soibelzon, L.H., 2019. Comparative osteology and functional morphology of the forelimb of Cyonasua (Mammalia, Procyonidae), the first South American carnivoran. Journal of morphology, 280(3): 446-470.

Tarquini, J., Soibelzon, L.H., Salas-Gismondi, R. and Muizon, C.d., 2020. Cyonasua (Carnivora, Procyonidae) from late Miocene of Peru shed light on the early dispersal of carnivorans in South America. Journal of Vertebrate Paleontology, 40(5) (5): e1834406. https://doi.org/10.1080/02724634.2020.1834406

Urbina, M. and Stucchi, M., 2005. Evidence of a fossil stork (Aves: Ciconiidae) from the late Miocene of the Pisco Formation, Peru. Boletin de la Sociedad Geológica del Perú, 100(2): 63-66.

Valenzuela-Toro, A.M., Gutstein, C.S., Suárez, M.E., Otero, R. and Pyenson, N.D., 2015. Elephant seal (Mirounga sp.) from the Pleistocene of the Antofagasta Region, northern Chile. Journal of Vertebrate Paleontology, 35(3): e918883. https://doi.org/10.1080/02724634.2014.918883

Varas-Malca, R., Salas-Gismondi, R., Ochoa, D. and DeVries, T.J., 2019. Filling The Gap In The History Of Otariid Seals From The Southeastern Pacific Ocean, North American Paleontological Convention (NAPC), Riverside, California.

Velez-Juarbe, J., Domning, D.P. and Pyenson, N.D., 2012. Iterative evolution of sympatric seacow (Dugongidae, Sirenia) assemblages during the past ~26 million years. PloS one, 7(2): e31294-e31294. https://doi.org/10.1371/journal.pone.0031294

Vermeesch, P., 2018. IsoplotR: A free and open toolbox for geochronology. Geoscience Frontiers, 9(5): 1479-1493. https://doi.org/10.1016/j.gsf.2018.04.001

Wood R.C., Johnson-Gove J., Gaffney E.S. and K.F., M., 1996. Evolution and Phylogeny of Leatherback Turtles (Dermochelyidae), with Descriptions of New Fossil Taxa: Chelonian. Conservation and Biology, International Journal of Turtle and Tortoise Research 2: 266-286.